Global Change Biology

Fire transforms effects of terrestrial subsidies on aquatic ecosystem structure and function

Journal:	*Global Change Biology*
Manuscript ID	Draft
Wiley - Manuscript type:	Research Article
Date Submitted by the Author:	n/a
Complete List of Authors:	Wall, Christopher; University of California San Diego, Spiegel, Cody; University of California San Diego, Ecology, Behavior, Evolution Diaz, Evelyn; University of California San Diego Tran, Cindy; University of California San Diego, Ecology, Behavior, Evolution Fabiani, Alexia; University of California San Diego Broe, Taryn; University of California San Diego Perez-Coronel, Elisabet; University of California San Diego Jackrel, Sara; University of California San Diego Mladenov, Natalie; San Diego State University, Civil Construction & Environmental Engineering Symons, Celia; University of California Irvine, Ecology and Evolutionary Biology Shurin, Jonathan; University of California San Diego, Section of Ecology, Behavior and Evolution
Keywords:	fire, plankton, productivity, aquatic, dissolved organic carbon, pyrogenic, trophic transfer
Abstract:	Fire can lead to transitions between forests and grassland ecosystems and trigger positive feedbacks to climate warming by releasing CO2 into the atmosphere. Climate change is projected to increase the prevalence and severity of wildfires. However, fire effects on the fate and impact of terrestrial organic matter (i.e., terrestrial subsidies) in aquatic ecosystems is unclear. Here, we performed a gradient design experiment in freshwater pond mesocosms adding 15 different amounts of burned or unburned plant detritus and tracking the chronology of detrital effects at 10, 31, 59, and 89 days. We show detrital effects from terrestrial subsidies displayed time- and mass-dependent, non-linear impacts on ecosystem function that influenced dissolved organic carbon, ecosystem metabolism (net primary production and respiration), greenhouse gas concentrations (carbon dioxide [CO2], methane [CH4]), and trophic transfer, and these impacts were shifted by fire treatment. Burning increased the elemental and organic composition of detritus (increasing %N, %P, %K), with cascading effects on ecosystem function. Fire magnified detrital effects on aquatic ecosystem metabolism by stimulating photosynthesis and respiration at intermediate detritus-loading and caused long-term destabilization and hypoxia at highest

	detritus-loading. Fire reduced detrital effects on dissolved organic carbon (DOC) and CO2 concentrations, while increasing autochthonous food source utilization and reducing the trophic transfer of 15N-labeled detritus into plankton biomass. Our results indicate the chemical transformation of plant detritus by fire alters the role of these ecosystems in processing and storing carbon. Wildfire may therefore induce shifts in ecosystem functions that cross the boundary between aquatic and terrestrial habitat.

Fire transforms effects of terrestrial subsidies on aquatic ecosystem structure and function

Christopher B. Wall[1]*, Cody J. Spiegel[1], Evelyn Diaz[1], Cindy Tran[1], Alexia Fabiani[1], Taryn Broe[1], Elisabet Perez-Coronel[1], Sara Jackrel[1], Natalie Mladenov[2], Ceila C. Symons[3], Jonathan B. Shurin[1]

[1]Department of Ecology, Behavior and Evolution, Division of Biological Sciences, University of California, San Diego, CA, USA

[2]Department of Civil Construction & Environmental Engineering, San Diego State University, CA, USA

[3]Department of Ecology, Behavior and Evolution, University of California, Irvine, CA, USA

Running title: Fire effects on aquatic ecosystems

* corresponding author: cbwall@ucsd.edu

Keywords: fire, plankton, productivity, aquatic, dissolved organic carbon, pyrogenic, trophic transfer

Abstract

Fire can lead to transitions between forests and grassland ecosystems and trigger positive feedbacks to climate warming by releasing CO_2 into the atmosphere. Climate change is projected to increase the prevalence and severity of wildfires. However, fire effects on the fate and impact of terrestrial organic matter (i.e., terrestrial subsidies) in aquatic ecosystems is unclear. Here, we performed a gradient design experiment in freshwater pond mesocosms adding 15 different amounts of burned or unburned plant detritus and tracking the chronology of detrital effects at 10, 31, 59, and 89 days. We show detrital effects from terrestrial subsidies displayed time- and mass-dependent, non-linear impacts on ecosystem function that influenced dissolved organic carbon, ecosystem metabolism (net primary production and respiration), greenhouse gas concentrations (carbon dioxide [CO_2], methane [CH_4]), and trophic transfer, and these impacts were shifted by fire treatment. Burning increased the elemental and organic composition of detritus (increasing %N, %P, %K), with cascading effects on ecosystem function. Fire magnified detrital effects on aquatic ecosystem metabolism by stimulating photosynthesis and respiration at intermediate detritus-loading and caused long-term destabilization and hypoxia at highest detritus-loading. Fire reduced detrital effects on dissolved organic carbon (DOC) and CO_2 concentrations, while increasing autochthonous food source utilization and reducing the trophic transfer of ^{15}N-labeled detritus into plankton biomass. Our results indicate the chemical transformation of plant detritus by fire alters the role of these ecosystems in processing and storing carbon. Wildfire may therefore induce shifts in ecosystem functions that cross the boundary between aquatic and terrestrial habitat.

Introduction

Positive and negative feedback between ecosystems and the atmosphere represent significant sources of uncertainty when forecasting future climate scenarios. Melting sea ice and permafrost, and the expansion of wildfire and biotic disturbances (e.g., forest insect outbreaks, invasive species), may liberate more carbon to the atmosphere and reduce the capacity for terrestrial and aquatic ecosystems to serve as carbon sinks, unleashing vicious cycles of climate and ecosystem instability that accelerate further warming (Fei et al., 2019; Hicke et al., 2012; Natali et al., 2021; Zheng et al., 2021). Fires liberate terrestrial carbon and produce greenhouse gasses (e.g., carbon dioxide [CO_2], methane [CH_4], nitrous oxide [N_2O]) and aerosols that shape the radiative balance of the atmosphere (Bowman et al., 2009). Globally, CO_2 emissions from wildfires contribute 1.8 Gt of C $year^{-1}$ to the atmosphere (2000-2019) (Zheng et al., 2021), equivalent to 5% of net carbon emissions in 2021 (34.9 $GtCO_2$) (Z. Liu et al., 2022). As atmospheric CO_2, climate models predict a combination of human behavior and land-use practices will act in positive feedback with rising global temperatures and anthropogenic climate change (Zheng et al., 2021) to increase the severity and frequency of wildfires (M. W. Jones et al., 2022; Y. Liu et al., 2010; Pausas & Keeley, 2021).

Wildfires are important disturbances that structure biological communities and shape the ecological properties and biogeochemistry of terrestrial (McLauchlan et al., 2020) and inland aquatic ecosystems (Bixby et al., 2015) and the oceans (Tang et al., 2021). Wildfires generate pyrogenic materials (e.g., smoke, ash, woody debris) that destabilize soils and increase the flux of nutrients and organic materials into inland and coastal waters (Larsen et al., 2009; Lewis et al., 2019). The deposition of pyrogenic materials as detritus and aerosols can alter the biogeochemistry in waterways and fluvial networks (Ball et al., 2021) and contribute to marine

phytoplankton blooms by increasing nutrient availability (Tang et al., 2021). The impact of fire disturbance on terrestrial systems depends on ecosystem type (i.e., wetland, grassland, riparian forest), fire severity and area burned, and can show both acute and sustained effects on ecosystem function (McCullough et al., 2019; Paul et al., 2022; Santos et al., 2019). Fire affects nutrient export and the retention by mobilizing nutrients (nitrogen [N] and phosphorus [P]) by producing partially combusted recalcitrant materials (pyrogenic or black carbon) (Bixby et al., 2015) that can have immediate and long term impacts on vegetation, soils, and watersheds (Dahm et al., 2015; Diemer et al., 2015; Rodríguez-Cardona et al., 2020). In burned stream areas, wildfires increased dissolved organic carbon (DOC), dissolved organic nitrogen, fine-sediments, and particulate organic matter (POM) relative to unburned reference streams (Minshall et al., 2001). Wildfire can increase erosion and detritus deposition in waterways, which can alter microbial metabolism and biogeochemical cycling (Bladon et al., 2008; Santos et al., 2019), reducing water quality, and contributing to low-O_2 conditions with lethal consequences for aquatic organisms (Dahm et al., 2015; Ramberg et al., 2010). As such, fire represents a disturbance that precipitates rapid changes in ecosystem services and biodiversity both on land and in water with implications for global carbon cycling and biosphere feedbacks to climate change (McCullough et al., 2019; McLauchlan et al., 2020).

Wildfires alter the fate and impact of terrestrial organic matter in aquatic ecosystems which provide both inorganic nutrients that support primary producers and organic substrates (i.e., dissolved organic matter [DOM]) for growth of heterotrophic microbes (Lennon, 2004), as well as humic organic compounds that absorb light and suppress photosynthesis (Solomon et al., 2015). For instance, burning can alter both the elemental stoichiometry and chemical composition of organic matter (plant litter and soils) (Butler et al., 2020; Pellegrini et al., 2021)

that impact the lability and susceptibility of organic matter to microbial and photochemical transformation/degradation (Lennon & Pfaff, 2005; Obernosterer & Benner, 2004; Solomon et al., 2015). These fire effects on organic material are known to propagate through forest food webs (Butler et al., 2021) and can also drive multi-year increases in nutrients and elemental concentrations in aquatic systems post-fire (Carignan et al., 2000). The chemical transformation of plant detritus by fire can shape the processing and decomposition of burned materials by heterotrophic microbes and macroinvertebrates (Rodríguez-Lozano et al., 2015), thereby altering the rate and efficiency of energy transfer through food webs. As a result, burned and unburned detritus may have distinct impacts on the metabolic balance and functioning of aquatic ecosystems that determine the fate of terrestrial organic matter and the biological properties of aquatic food webs.

Natural (i.e., ponds, lakes, rivers, and streams) and artificial inland waters (i.e., reservoirs) account for 90% of the freshwater surface area globally and are significant sources of CO_2 and CH_4 to the atmosphere (Pilla et al., 2022). The influx of terrestrial subsidies (i.e., various forms of plant detritus) into aquatic ecosystems support net heterotrophy and can increase the emissions of greenhouse gasses (Lennon, 2004). The combined recalcitrant and light attenuating properties of terrestrial-DOC can reduce rates of nutrient turnover (Jones & Lennon, 2015) and the efficiency by which essential substances (i.e., carbon, nitrogen, fatty acids) are transferred between phytoplankton and zooplankton (Karpowicz et al., 2021), thereby affecting lake ecosystem function and nutrient cycling. Fluxes of allochthonous inputs after wildfires and floods may lead to enhanced browning, where silt and organic compounds further affect light attenuation, reduce chlorophyll (Whitney et al., 2015) and increase respiration, resulting in hypoxic or anoxic conditions (Dahm et al., 2015). These effects can further suppress

microbial degradation and shift carbon cycling and turnover by increasing carbon storage in sediments (Isidorova et al., 2016). Considering the long residence times (months to years) in lakes and ponds, these systems may be particularly vulnerable to fire disturbance relative to other waterways (McCullough et al., 2019); however, a comprehensive understanding of fire effects (and their chronology) on these inland waters is lacking.

Here, we performed a gradient-design mesocosm experiment to test the effects of terrestrial subsidies on experimental pond ecosystems and whether these effects were altered by burning. We ask how wildfire affects the fate and impact of terrestrial production in aquatic ecosystems and potential critical thresholds in the loading of plant material. Thirty 400L pond mesocosms received 15 different amounts of either burned or unburned plant detritus (sage and willow). We measured ecosystem metabolism by the amplitude of daily cycles in dissolved oxygen concentrations, and concentrations of dissolved greenhouse gasses (CO_2, CH_4) at the water surface. Considering the potential for fire to alter the metabolic balance and the assimilation and transfer of energy in food webs (Spencer et al., 2003), we used burned and unburned sage labeled with ^{15}N to measure the incorporation of the ^{15}N into plankton biomass (i.e., % sage-derived ^{15}N), hereafter referred to as trophic transfer. We predicted detrital loading would have non-linear (hump-shaped) effects on ecosystem metabolism, stimulating production and respiration at low levels due to fertilization but suppressing them at higher levels where oxygen and light were depleted. Because fire transforms the stoichiometry and organic chemistry of plant detritus, we predicted these non-linear functions to vary between the burned and unburned allochthonous sources, reducing ecosystem productivity and trophic transfer.

Materials and Methods

Experimental design

Thirty experimental mesocosms (400 L) were used to test the influence of plant detritus loading and burning effects on aquatic ecosystems. Fifteen mesocosms received unique amounts of either burned or unburned plant detritus, with two control tanks receiving no plant material. We used a regression design to test for non-linear response surfaces in the dependent variables. In this design, fifteen mesocosms contained gradually increasing quantities of either burned or unburned plant material ranging from 0 to 400 g of dried plant biomass, with stepwise increases in plant material ranging from 11 - 150% from one treatment level to the next. This range in detrital loading was chosen based on preliminary tests on loading effects on water quality and to optimize the number or mesocosms within each treatment group. To account for water loss due to evaporation, water levels in the mesocosms were maintained by adding water from an adjacent 400 L reservoir tank on a weekly basis. With the exception of mixing caused by periodic water additions, no attempts were made to stimulate flow, turnover, or to disturb detritus that settled at the bottom of tanks.

Each mesocosm was filled with municipal water (27 October 2021) and stocked with a concentrated mixture of live phytoplankton and zooplankton (> 63 μm mesh) collected from vertical tows at Lake Murray and Lake Miramar, San Diego, CA (28 October, 5 November 2021). A sample of this concentrated plankton material was filtered onto a pre-combusted (2 h, 550 °C) 0.7 μm GF/F filter and dried (60 °C) for isotope analysis (see below). We used plant biomass from two shrubs native to southern California and abundant in western North America: *Salvia leucophylla* (Greene) (hereafter, sage) and *Salix lasiolepis* (Benth.) (hereafter, willow). Twenty-three sage plants were purchased from a local nursery (9 June 2021) and grown in a 1:1

161 soil:vermiculite mixture in pots at the University of California San Diego Research Field Station
162 (La Jolla, CA).
163 On 24 June 2021 sage plants were watered with a single pulse (100 ml) of 0.021 M
164 $^{15}NH_4Cl$ in distilled water added to the base of the plants, elevating soil ^{15}N abundance to an
165 estimated 6.4 atom-%. Sage plants were grown for 60 days until harvest on 9 September 2021.
166 Willow plant material was collected on 6 October 2021 from the University of California
167 Dawson Los Monos Reserve (Buena Vista, CA).
168 Sage and willow leaves and stems (< 2 cm diameter) were kept separate and air dried in a
169 greenhouse for 24 h, followed by 24 h in a drying oven (45 °C). Once dried, plant biomass was
170 cut into small pieces (< 10 cm) and divided into groups that either remained unburned or were
171 exposed to fire. To simulate the non-uniform effects of wildfire on plant biomass, we exposed
172 burned plant material to varying degrees of burning at low and high burn severity, determined
173 through visual assessment of burning. Plant material (leaves and stems) was loaded into 75 L
174 aluminum containers and flamed with a handheld butane torch. To control the extent of burning,
175 flames were extinguished with aluminum lids. The low and high severity burned plant materials
176 were pooled according to plant species. In total ~2 kg of burned and unburned material was
177 harvested for both sage and willow.
178 We analyzed plant isotopic ratios and elemental composition to evaluate the effects of
179 fire on the starting plant materials added to mesocosms and the contribution of isotope tracer
180 (i.e., ^{15}N) to aquatic food webs. Leaves (~ 5 mg) from each species (sage and willow) and
181 treatments (burned and unburned) were separately ground and packed in tin capsules for C and N
182 isotope analysis (see below). Percent concentrations of nitrogen (N), sulfur (S), phosphorus (P),
183 potassium (K), and zinc (Zn) were measured separately for leaves and woody stems of both

184 burned and unburned sage and willow plant biomass at A&L Western Laboratories (Modesto,
185 CA). A dried sample of plant materials for each species was also stored for stable isotope
186 analysis (see below).
187 Burned and unburned plant materials for each species were weighed and packed into leaf
188 litter bags (25 x 15 cm nylon bags of 250 μm mesh size) to reduce leaf detritus transfer among
189 tanks and increase negative buoyancy, while also allowing for invertebrate micrograzing and
190 water flow. Each experimental mesocosm contained an equal mass of sage and willow for their
191 respective fire-treatment (burned or unburned material), such that the lowest and highest plant
192 biomass treatments (5 g and 400 g dry biomass added) received 2.5 or 200 g of both willow and
193 sage, respectively. On 5 November 2021, litter bags containing either burned or unburned sage
194 and willow were placed into respective mesocosms; two tanks were left as controls where
195 plankton were stocked but no plant materials were added.
196
197 *Sampling design and response metrics*
198 Mesocoms were sampled five times during the experimental period: once at the start of the
199 experiment before plant materials were added (3 November 2021, Day-0), and four times after
200 the addition of plants on 5 November 2021: Day-10 (15 November 2021), Day-31 (6 December
201 2021), Day-59 (3 January 2022), and Day-89 (2 February 2022).
202 Environmental parameters (temperature, dissolved oxygen, pH, conductivity) were
203 measured throughout the study using a YSI Pro-Plus handheld multiparameter water sensor (YSI
204 Inc., Yellow Spring, OH) calibrated against certified standards. During each discrete sampling
205 period, measurements of dissolved oxygen concentration were made three times (dawn-dusk-
206 dawn) to calculate net primary productivity (NPP) and respiration (R).

Isotope values were assessed in seston (< 63 µm, consisting of particulate organic material [POM] and organisms [i.e., phytoplankton, rotifers]) and zooplankton (> 63 µm) at two time points (Days-10 and 31). Water samples were collected in each mesocosm with a 1-m integrated water sampler, filtered through a 63 µm mesh separating the zooplankton and seston (hereafter, POM), and each fraction was filtered onto a pre-combusted (2 h, 550 °C) 0.7 µm GF/F filter. Filters were wrapped in pre-combusted aluminum foil, frozen (-20 °C), and freeze-dried. Once dried, the loaded biomass was scraped from the surface of the GF/F filter using a razor blade into a mortar and either cut with scissors or ground with a pestle before being packed into tin capsules for analysis. Approximately 10% of samples were run in duplicate. In addition to plankton and POM, dried leaves from (1) burned and unburned sage and willow and (2) the > 63 µm concentrated plankton (~1.5 g) from Lake Murray were ground and sampled for isotope analyses (n = 4-7 each). Measurement of nitrogen stable isotope values ($\delta^{15}N$), carbon and nitrogen molar concentrations (C:N), and atom percent (atom-% ^{15}N) were made using an elemental analyzer-isotope ratio mass spectrometer (EA-IRMS) at the University of California Davis Stable Isotope Facility. Isotope values for non-enriched, natural abundance samples are reported in delta values (δ) using per mil (‰) notation relative to atmospheric N_2 standards (air). Enriched samples are reported in absolute abundance of ^{15}N (i.e., atom-% ^{15}N). Reproducibility of isotope abundance measurements was always within ± 0.2 ‰.

The production and efficiency of energy transfer through food webs is often represented as inorganic carbon fixed by phytoplankton and incorporated in zooplankton biomass (Karpowicz et al., 2021); however, the assimilation and trophic transfer of nitrogen can also serve as an effective proxy for carbon (Barneche et al., 2021). To test this assumption, we used plankton C:N molar concentrations at both time sampling periods (Days-10 and 31) and across

all mesocosms in both treatments to verify nitrogen assimilation was proportionate to carbon across times and treatments (i.e., no systematic change in C:N values) and within each plankton size fraction. We used a linear model to validate this assumption and found no effects of treatment (p=0.915) or sampling period (Days-10 and 31) (p=0.783) on plankton C:N, and C:N was higher in POM/phytoplankton (< 63 μm) than zooplankton (> 63 μm), as has been shown previously (p<0.001) (Barneche et al., 2021). Therefore, we use $\delta^{15}N$ values of the two plankton size fractions as a measure of incorporation of sage biomass into the aquatic food web. $\delta^{15}N$ values of ^{15}N-labeled sage (nitrogen source 1 [$\delta^{15}N$ of 296 ‰] a proxy for allochthonous nutrients) and the stock zooplankton mixture at natural abundance (nitrogen source 2 [$\delta^{15}N$ of 11 ‰], a proxy for autochthonous nutrients) were used in a two member mixing model to determine the trophic transfer of nitrogen through aquatic food webs (Post, 2002). We used the mixing model to calculate the % sage-derived ^{15}N (hereafter, sage-^{15}N) as a proxy for terrestrial contributions to plankton biomass. Considering, $\delta^{15}N$ values of non-labeled willow ($\delta^{15}N$ of 13 ‰) overlap with those of the plankton mixture, mixing models represent the contribution of ^{15}N entering plankton from sage alone and are not meant to estimate full flow of plant-derived N into higher trophic levels.

Water samples for DOC and total dissolved nitrogen (TDN) were collected at five timepoints using an integrated water sampler placed randomly across each tank; total dissolved phosphorus (TDP) was measured at one time point (Day-31). DOC and TDN water samples were filtered (pre-combused 0.7 μm GF/F filters), stored in pre-combusted borosilicate amber vials, and acidified (37% HCl) to a pH of 3. Mesocosm DOC and TDN were measured in the WIRLab at San Diego State University using a high temperature combustion method (Shimadzu TOC-L Total Organic Carbon and Total Nitrogen Analyzer) calibrated with potassium hydrogen

phthalate standards (1 - 50 mg C/L, 1 - 10 mg N/L). Approximately 10% of samples were run in duplicate, with standard deviations of repeat-measurements falling within 10% of mean values. TDP was measured at the University of Hawai'i Hilo Analytical Laboratory on a Lachat QuikChem 8500 series 2 Flow-Injection Analyzer using USGS I-4650-03 for external digestion and US-EPA method 365.3 for phosphorus analysis (detection limit of 3.1 µg/L P).

Greenhouse gas concentrations

Samples for carbon dioxide (CO_2) and methane (CH_4) greenhouse gasses were collected from each tank on Days-0, 10, 31 and 59 of the experiment using the headspace method (Perez-Coronel et al., 2021; Sobek et al., 2003). Background concentrations of CO_2 and CH_4 in ambient air were collected at each sampling day by collecting 12 mL of air in evacuated Exetainers (Labco Limited). Day-0 ambient air CH_4 concentrations were determined to be outliers and were discarded, being replaced with ambient CH_4 concentrations for Day-10. Tank water temperatures were recorded and for each tank, 35 mL of surface water (0.1 m depth) was collected in a sterile 60 mL syringe. An additional 25 mL of ambient air was collected into the same syringe. The syringe containing water and air was shaken for 2 minutes to reach equilibration and air was then injected into evacuated Exetainers for CO_2 and CH_4 quantification. Samples were stored upside down at room temperature, and sent for analysis within three weeks to the University of California Davis Stable Isotope Facility.

Analysis of atmospheric CO_2 was performed using a Thermo Scientific GasBench II coupled to a Thermo Finnigan Delta Plus XL isotope-ratio mass spectrometer. Analysis of atmospheric CH_4 was performed on a Thermo Scientific GasBench II + PreCon trace gas concentration system coupled to a Thermo Scientific Delta V Plus isotope-ratio mass

spectrometer. Molar concentrations of CO_2 and CH_4 in water were calculated based on headspace concentrations of CO_2 (Weiss, 1974) and CH_4 (Yamamoto et al., 1976) and gas solubilities using the appropriate temperature and atmospheric pressure corrected Henry's constant and accounting for the amount of CO_2 or CH_4 added by ambient air (Kokic et al., 2015). Unlike CH_4, CO_2 undergoes dynamic chemical equilibrium with multiple carbonate species and in the absence of measurements of total alkalinity or dissolved inorganic carbon, quantification of CO_2 concentration using the headspace method can lead to poor resolution in undersaturated samples at low pCO_2 (Koschorreck et al., 2021). Therefore, CO_2 concentration measurements herein should be considered a relative measure, with the goal of comparing differences among treatments in response to plant detritus loading and burning.

Statistical analysis

A series of linear models and non-parametric tests were used to evaluate differences in $\delta^{15}N$ values and C:N ratios across starting materials (willow, sage, plankton; leaves vs. stems) and effects of burning treatments on starting plant materials. Using pooled values for burned and unburned leaves, Mann-Whitney *U*-tests evaluated differences in $\delta^{15}N$ and C:N between the plant materials (^{15}N-labeled sage versus non-labeled willow leaves) and non-labeled materials (willow versus the plankton stock). Burning effects on $\delta^{15}N$ and C:N in sage leaves and willow leaves were evaluated in separate one-way linear models. A two-way linear model was used to test treatment (burned, unburned) and plant material type (leaves, stem) effects on sage and willow biomass (nitrogen (%N), potassium (%K), phosphorus (%P), sulfur (%S), zinc (Zn ppm)), with ANOVA tables generated using Type III sum of squares in the *car* package (Fox et al., 2019).

The effects of treatment (burned and unburned) and plant detritus loading on the response variables were analyzed using generalized additive models (GAMs) in the *mgcv* package in R (Wood, 2011). Each time point was analyzed individually to account for the dynamic changes in response metrics over the course of the experiment since full models (i.e., the inclusion of all time points) introduced extreme concurvity. Within each time point, we applied GAMs in a model selection framework that compared three models: the 'simplest' model including only a single global smoother fit to all data; a model with a global smoother and a parametric 'Treatment' term, allowing different intercepts for burned and unburned treatments; and a more complex model with a factor-smooth term which provided different smoothers for each treatment in addition to a parametric term for treatment-specific intercepts. This approach allowed us to evaluate the relationship between response variables and plant biomass gradient with the hypotheses that these relationships were non-linear and either offset according to treatments and/or exhibited distinct treatment-specific structure (Pedersen et al., 2019).

Candidate models were compared using Akaike Information Criterion (AIC), and models with the lowest AIC value selected. GAMs were inspected for model concurvity using the 'concrvity' function in the package *gratia* (Simpson, 2022). Model fits were assessed using 'gam.check,' with analysis of variance (ANOVA) tables generated using 'anova.gam' in the *mgcv* package to provide Wald tests of significance for parametric and smooth terms. In all cases, differences between burned and unburned treatments were illustrated by plotting the "difference smooth" using 'plot_difference' in *tidymv* (Coretta et al., 2022), which calculates the differences between smooths of two conditions and determines regions of significance as areas where *s*(treatment 1) - *s*(treatment 2) is greater than zero and does not include treatment-smooth confidence intervals. In models testing ^{15}N-enrichment and the contribution of sage-^{15}N to

plankton, size fraction (i.e., <63 μm POM and >63 μm zooplankton) was also included as a parametric term for model selection. Plankton C:N were visualized using a GAM with size fraction as both a main effect and a factor-smooth term.

Results

Elemental analyses

We observed differences in elemental concentrations in plant material among species, tissue types, and burning treatments, although the largest differences being between species and plant parts (*Supplemental Materials*, Table S1 and S2). For sage, burning reduced leaf %N but increased stem %N, and increased %K in both leaf and stem samples (*Supplemental Materials*, Figure S1). Willow showed greater and more consistent shifts in elemental composition, with burning increasing %N, %P, and %K in both leaf and stem samples and increasing %S and Zn ppm in leaves alone (*Supplemental Materials*, Figure S1).

Dissolved organic carbon

Prior to the addition of plant material DOC concentrations were low, averaging ~ 3 mg/L across all mesocosms. Following the addition of plant material, DOC increased to ~ 60 mg/L in highest treatments (Figure 1). Detritus loading had significant non-linear effects on DOC concentrations throughout the experiment, and DOC concentrations showed distinct patterns among burned and unburned treatments. This relationship was strongest early in the experiment when DOC concentration was highest (Days 10 and 31) but was reduced in subsequent samplings as DOC declined (Figure 1). The rise in DOC with detrital loading also differed among burned and unburned treatments at the first three time points (Days 10, 31, 59) (*Supplemental Materials*,

Figure S2), as indicated by best-fit model AIC (*Supplemental Materials*, Table S3) and differences between factor smoothers (*Supplemental Materials*, Table S4). DOC was lower in the burned than unburned treatment in mid-range plant additions (~100 - 300 g) at Day-10 and Day-31 (~200 - 300 g); however, DOC was highest in the burned 400 g treatment at Day-31 and remained elevated in burned tanks (~250 - 400 g) through Day-59 (Figure 1 and *Supplemental Materials*, Figure S2). By the last sampling period (Day-89), DOC still showed a positive relationship with plant detritus loading, although this effect was small (total DOC range 4 - 12 mg/L) and equivalent between burning treatments (Figure 1 and *Supplemental Materials*, Figure S2).

Total dissolved nitrogen and phosphorus

The addition of plant material had significant non-linear effects on TDN that persisted through Day-89 (*Supplemental Materials*, Figure S3). This shape of the non-linear relationship was similar between burned and unburned treatments at Day-10. Subsequently, burned and unburned treatments diverged and maintained statistical differences through Day-89. TDN tended to be lower in burned tanks at Day-31 (p=0.053) but was notably higher in high-range (> 200 g) burned treatments at Day-59 and mid-range treatments (~ 100-250 g) at Day-89 (*Supplemental Materials*, Figure S4 and Table S3 and S4). Phosphorus (as TDP) in treatment water was only measured once during the experiment (Day-31). Similar to DOC at Day-10, TDP increased in both treatments with detritus loading and was higher in burned vs. unburned tanks especially at high-detritus loading tanks (*Supplemental Materials*, Figure S5 and Tables S3 and S4).

Net primary productivity and respiration

Dissolved oxygen (DO as % O_2) measurements showed consistent patterns among paired dawn measurements (separated by 24 h) in each time point (*Supplemental Materials*, Figure S6). Percent O_2 showed considerable change over time and treatments (*Supplemental Materials*, Figure S7, model fits in Tables S5 and S6). Relative to unburned tanks, % O_2 was consistently higher in mid-range burned treatments and lower in burned treatments receiving the highest plant material (400 g) (*Supplemental Materials*, Figure S6).

NPP (as Δ % O_2) showed a significant non-linear relationship with plant biomass across all four time points. NPP was greater in burned relative to unburned tanks through Day-59 (Figure 2A and *Supplemental Materials*, Table S7 and S8). At Day-10, NPP exhibited an exponential decline with highest values in low-plant biomass treatments that also tended to be higher in burned tanks with low-plant biomass (Figure 2A and *Supplemental Materials* Figure S8A). By Day 31, NPP had stabilized across the plant-biomass gradient but a negative relationship between NPP and biomass loading remained (Figs. 2A and *Supplemental Materials*, Figure S8A), and NPP was higher in burned tanks (p=0.007). This pattern continued through Day-59, with an increasing unimodal relationship where highest NPP was observed in mid-range tanks (100-200g) and burned tanks (p=0.012) (*Supplemental Materials*, Table S8). By Day-89, NPP in unburned tanks was flat across the plant biomass gradient (p=0.327) (Figure 2A), while NPP in burned tanks continued to show an unimodal relationship with plant biomass (p=0.020). NPP at Day-89 was significantly lower in burned tanks receiving >250 g plant material compared to unburned tanks (Figure 2A and *Supplemental Materials*, Figure S8A).

Respiration (R) mirrored NPP and was greatest (most negative) in low-biomass treatments throughout the experiment. We observed significant non-linear associations between R and plant biomass at Day-10 that did not differ between treatments (p=0.229) (Figure 2B);

however, by Day-31 R was offset by treatment-level intercepts, with an overall significant effect of treatment driving greater rates of respiration (more negative) in burned tanks (p=0.019) (*Supplemental Materials*, Table S7 and S8). Treatment-specific non-linear effects of plant addition on R were found for both burned and unburned treatments at Day-59 (p<0.001) and burned tanks alone at Day-89 (p=0.004). Significant differences between treatment R were in mid-range burned tanks (~100-225 g) at Day-59 where R was greatest, and in high-range treatments (300-400 g) at Day-89 where rates of R were reduced (least negative change in O_2) (Figure 2B, and *Supplemental Materials*, Figure S8B).

Plankton ^{15}N-labeling

We assessed trophic transfer using the integration of sage-^{15}N into zooplankton biomass as a proxy for the input of plant nutrition to consumers. Analysis of plant materials before being added to mesocosms showed isotope labeling (i.e., ^{15}N) increased the $\delta^{15}N$ isotope values of both burned-and-unburned sage (p<0.001), and burning treatment did not affect leaf $\delta^{15}N$ values for sage (p=0.423) or willow (p=0.485) (see *Supplemental Results*, Figure S9 and Table S9). Isotope mixing models showed a significant effect of plant addition and burning on the trophic transfer (% sage-^{15}N) in plankton at Day-10 and Day-31 (p<0.001) (*Supplemental Materials*, Tables S10 and S11), with overall lower % sage-^{15}N in burned relative to unburned treatments (Figure 3); no difference between plankton size fractions (< 63 μm, > 63 μm) was observed at either time point (p≥0.196) (*Supplemental Materials*, Table S11). At Days-10 and 31, both treatments showed a non-linear relationship between % sage in plankton and detritus loading (p<0.001) (*Supplemental Materials*, Table S11), where plankton % sage-^{15}N increased with plant biomass following a saturating relationship. However, an asymptote for % sage-^{15}N in the

414 burned treatment occurred at lower plant addition levels in the burned treatment at Day-10 (~300
415 g of plant biomass). At Day-31 % sage-^{15}N substantially declined in 400 g burned treatment
416 (Figure 3). Overall, burning decreased trophic transfer and the incorporation of sage-^{15}N into
417 plankton in treatments receiving 50-400 g of material at Day-10 and ~ 75-125 g and >300 g at
418 Day 31 (*Supplemental Materials*, Figure S10). These results show a greater integration of plant-
419 derived nitrogen assimilated and transferred in the plankton food web in unburned treatments
420 and a pronounced drop off in trophic transfer and greater autochthonous nutrition in burned
421 treatments as detrital loading increased (Figure 3).
422
423 *Greenhouse gasses*
424 Prior to the addition of plant materials (Day-0), CO_2 concentrations in tanks ranged from 20 - 40
425 µM (Figure 4A). After the addition of plant material, CO_2 concentrations had increased to > 300
426 µM CO_2 in the highest biomass tanks by Day-10. Significant relationships between CO_2
427 concentrations and plant material were found for both burned and unburned treatments at all time
428 points (p<0.001). CO_2 concentrations were consistently higher in the unburned relative to
429 burned tanks in treatments receiving 100 - 325 g plant material at Days-10, 31, and 59
430 (*Supplemental Materials*, Figure S12 and Table S12 and S13). However, CO_2 concentrations
431 were highest in the burned treatments receiving 400 g plant material at Days-31 and 59 (Figure
432 4A).
433 In contrast to CO_2, the concentrations of CH_4 increased through time but were less
434 impacted by treatments or plant biomass (Figure 4B). Treatment effects were most apparent at
435 Day-10, where CH_4 concentrations showed a non-linear relationship for unburned tanks only
436 (p=0.001) and were higher in unburned tanks relative to burned tanks receiving >250 g of plant-

biomass (Figure 4B and *Supplemental Materials*, Figure S12). No relationship between CH_4 concentrations and plant-biomass or treatment was seen at Day-31 (p=0.659), although burned tanks tended to have higher CH_4 concentrations in burned tanks at Day-59 (*Supplemental Materials*, Figure S12 and Table S13).

Discussion

Our results show that the fire functionally alters the fate and impact of terrestrial organic subsidies in aquatic ecosystems and these impacts show non-linear dependencies linked to the quantity of terrestrial material introduced. The degradation of plant material in aquatic systems liberates nutrients and increases organic carbon (Blanchet et al., 2022) which can stimulate production under low detrital-loading by supplying limiting nutrients (Solomon et al., 2015). However, high detrital-loading led to light attenuation and can suppress aquatic primary production and respiration due to light absorption and oxygen depletion (Solomon et al., 2015) and harm ecosystem stability by perturbing rate of nutrient turnover (Jones & Lennon, 2015). Our results show that, in addition to fire impacts on terrestrial ecosystems, fire also shifts the metabolism, trophic transfer, and greenhouse gas production of aquatic systems. Burning enhanced the impact of detrital loading on ecosystem production and respiration, and dampened its effects on trophic transfer to plankton consumers. While burned treatments had greater NPP and autochthony, which led to lower CO_2 concentrations, CH_4 was higher in the burned treatment at the end of the experiment, suggesting wildfires may act to alter the GHG emissions from lentic systems. Therefore, more frequent, and intense wildfire may alter the capacity of aquatic systems to store, transform and exchange carbon with the atmosphere.

We observed increased terrestrial material and DOC to drive unimodal effects on ecosystem metabolism as tanks transitioned from nutrient- to light-limitations (Jones & Lennon, 2015; Solomon et al., 2015). Burning magnifies these patterns, with greater rates of system production and respiration at intermediate loading (Figure 2). At high detrital-loading (> 250g) burned tanks showed chronic destabilization with lower NPP, R, and DO after ~ 90 days (Figure 2, S6). Burning chemically transforms plant biomass (Butler et al., 2021) in ways that alter the feedbacks that link aquatic ecosystems to the metabolism, storage, and processing of terrestrial productivity. Wildfire impacts to aquatic ecosystems can persist for decades (Rodríguez-Cardona et al., 2020) but are especially dynamic in the first 5 years post-fire (Rust et al., 2018). Indeed, over the short period of our experiment (~ 90 d) we observed substantial temporal variability in water quality and productivity, suggesting a critical transition between terrestrial loading/DOC concentrations and the stimulatory effect of limiting nutrients on aquatic productivity (Stetler et al., 2021). These results suggest that positive impacts of fire on liberating dissolved organic and inorganic nutrients (e.g., N, P, DOC) (Hampton et al., 2022) and stimulating water column production at low and intermediate loadings gives way to tipping points where aquatic ecosystems are driven to dystrophic states under conditions of high biomass introduction. Fire also reduced both GHG concentration and the transfer of detritus (plant-derived nitrogen) to higher trophic levels (Figs. 3, 4). Therefore, accounting for feedback between wildfire and aquatic productivity and CO_2 concentration from freshwater ecosystems may be critical to a complete accounting of the role of fire in the global carbon cycle (Lasslop et al., 2019; D. Liu et al., 2022; Pilla et al., 2022).

The impacts of fire and terrestrial subsidies in our mesocosm experiment significantly affected aquatic ecosystem function, however, these effects showed distinct temporal patterns

related to time-since-disturbance (i.e., plant material introduction) and the amount of plant material added. For instance, terrestrial loading led to rapid, non-linear increases in DOC and CO_2 concentrations at Day 10 that reduced aquatic NPP and R to near zero as detritus loading increased. The non-linear relationship between detritus loading and DOC concentration indicates that organic carbon tended to be respired and released as CO_2 at intermediate concentrations, but to accumulate in the water column at the highest loading levels. Bacteria actively respire terrestrial-DOC in lakes, and bacterial contributions to productivity and respiration increase with DOC loading (Jones & Lennon, 2015). However, little of this respired terrestrial-DOC (i.e., bacterial pathway) is transferred to higher trophic levels compared to terrestrial particulate organic carbon (Cole et al., 2006). Elevated microbial respiration under increased detrital-loading contributed to hypoxia (Figure S6), which reduced the efficiency of biological degradation of organic material at the highest loading levels. A companion study (Spiegel et al., in review) found that microbes were responsible for more decomposition than photodegradation in our experiment, and that the highest rates of DOC decomposition occurred at intermediate concentrations. The saturating relationship between detrital loading and CO_2 concentrations also indicates that organic carbon was mineralized at slower rates at the highest concentrations where DOC accumulated and DOC respiration was lower in burned treatments (Figure 4), possibly due to fire-effects on DOC composition such as increased aromaticity. Over time, a unimodal pattern relating terrestrial inputs with ecosystem metabolism emerged, and by Day-31 declines in DOC and CO_2 concentrations were matched with greater rates of NPP and R with distinct non-linear relationships across the plant-biomass gradient between the burned and unburned treatments. These patterns show that rising inputs of terrestrial detritus into aquatic systems – a global phenomenon known as "browning" (Blanchet et al., 2022) – produce non-

505 linear feedbacks where both respiration and oxygenic primary production are stimulated by
506 terrestrially-derived nutrients and organic compounds at low and intermediate levels, but
507 suppressed by a combination of hypoxia, light limitation, and greater aromaticity at the highest
508 levels (Jones & Lennon, 2015).

509 Burning altered the shapes of the non-linear functions between terrestrial loading and
510 carbon dynamics and their evolution over time. Tanks receiving burned plant material had
511 significantly higher NPP than those with unburned material (Days-10, 31, 59) and R (Days-31,
512 59) and this effect was most pronounced at intermediate loading treatments. The greater
513 stimulation of ecosystem metabolism – primarily NPP – in burned treatments may be a result of
514 modest increase in limiting nutrients (%N, %P, %K, %S, %Zn) (*Supplemental Materials*, Figure
515 S1) or greater consumption of terrestrial-DOM by heterotrophic bacteria in burned tanks
516 releasing inorganic substances that favor autochthonous nutrient pathways (Jones, 1992; Jones &
517 Lennon, 2015). However, at high detrital-loading, dissolved phosphorus accumulated and this
518 effect was accentuated by burning (Figure S5), indicating a reduction of energy transfer across
519 trophic levels (Jones & Lennon, 2015) – possibly due to a combination of fire-induced changes
520 in DOC chemistry (increased aromaticity) (Spiegel et al, in review; Hampton et al., 2022), plant
521 polyphenols affecting enzyme activity (Hättenschwiler & Vitousek, 2000), and nutrient cycling
522 between autotrophic and heterotrophic microorganisms (Cole et al., 1988).

523 Greenhouse gasses also showed distinct fire effects later in the experiment, with burned
524 tanks exhibiting both lower (intermediate detrital-loading) and higher (high detrital-loading) CO_2
525 than unburned tanks at Days-31 and 59. Overall lower CO_2 concentrations in the burned
526 treatment at intermediate detrital-loading agrees with greater NPP in these tanks relative to the
527 unburned tanks. CH_4 concentrations increased four-fold across time in all tanks and were higher

in the burned treatment at the end of the experiment. Natural ponds and lakes account for 67% of CH_4 emissions from inland waters (Pilla et al., 2022), and the progressive rise in methane across our experiment may be the result of an increase in anaerobic methanogenesis localized within the detritus mesh bags as well as aerobic methanogenesis produced during bacterial photosynthesis (Perez-Coronel & Beman, 2022). The trend for higher CH_4 in the burned-detritus mesocosms at the end of the experiment, may likewise relate to greater autochthony and NPP in burned tanks also acting to stimulate bacterial methanogenesis. These results show fire may work in feedback with warming to increase NPP and draw down CO_2 in lentic systems which may favor CH_4 production. Taken together, these results show that the chemical transformation of terrestrial plant biomass by fire can lead to changes in the functioning of aquatic ecosystems, their metabolism, and the concentration of greenhouse gasses, and these effects depend both on the loading of terrestrial subsidies, their quality, and time since disturbance.

Increasing plant detritus increased DOC and other humic compounds that limited primary production and resulted in greater reliance of heterotrophic zooplankton on terrestrial resources. Zooplankton can utilize terrestrial organic carbon (t-OC), although the benefits of t-OC for zooplankton nutrition and growth is debated (Brett et al., 2009; Cole et al., 2011; Kelly et al., 2014). Relative to autochthonous nutrition, t-OC is low in nutritional quality due to high C:P and low unsaturated fatty acids (Brett et al., 2009). In natural lakes increasing t-OC and allochthony were found to reduce zooplankton production (Kelly et al., 2014). Greater consumption of recalcitrant carbon and an inefficient microbial loop (Cole et al., 2002) may explain lower zooplankton production and rates of nutrient transfer across trophic levels where t-OC is high. We observed the percent sage-^{15}N in two zooplankton size fractions to increase with detrital-loading and to be reduced in burned treatments; thus burning reduced trophic transfer of

plant N to higher trophic levels (Figure 3). While mixing model values represent the relative contribution of sage as a terrestrial resource to plankton, they do not represent full accounting of terrestrial inputs due to the added contribution of willow (at natural isotope abundance). Plant-derived N incorporation in zooplankton depended on the interaction between the detrital-loading and burning treatments. The saturating kinetics of this relationship show the assimilation of plant derived nitrogen to zooplankton increased proportionally as NPP decreased, supplying nutrients up to the highest loading levels where trophic transfer was markedly reduced. This effect was most notable in the burned treatments where zooplankton contained less sage-^{15}N than in the unburned treatment. Greater utilization of algae/autochthonous versus plant detritus/allochthonous food sources was also observed in macroinvertebrates and fishes in post-fire (< 5 y) streams, possibly due to fire reducing tree canopies and increasing light availability (Spencer et al., 2003). Therefore, fire may impact aquatic food webs by transforming the elemental composition of detritus and abiotic traits (i.e., terrestrial- and in-water shading, temperature [Barneche et al., 2008) important for ecosystem metabolism and trophic transfer. These effects can drive both short- and long-term changes in productivity, feeding behavior, and the transfer of energy in food webs.

We observed lower DOC (Figure 1) and higher NPP (Figure 2) in burned tanks to also coincide with a greater proportion of autochthonous nutrition and less plant-derived nutrition (using % sage-^{15}N as a proxy) in zooplankton compared to unburned treatments. In a companion study, (Spiegel et al. in review) decomposition (% mass loss) in burned sage was twofold greater than burned willow after ~90 d, but the decomposition of burned and unburned sage was largely equivalent across the detrital-loading gradient. Therefore, lower % sage-^{15}N in burned treatments overall and the marked decline at high detrital-loading, is likely not driven by

574 difference in rates of ^{15}N release from burned/unburned sage, but instead changes in dissolved
575 compounds, their lability, and composition (e.g., aromaticity) (Hampton et al., 2022; Rodríguez-
576 Cardona et al., 2020). Overall, this pattern indicates that the effects of fire on biogeochemistry,
577 microbial communities, and ecosystem metabolism are intimately related, and fire affects the
578 trophic transfer of detrital nutrients to top consumers through alternate energy pathways.

579 Our study suggests that a complete accounting of the impact of wildfire on the global
580 carbon cycle must include feedbacks to the functioning of aquatic ecosystems. Inland waters
581 transform and store carbon in their sediments at rates comparable to the global oceans (Ward et
582 al., 2017). Lakes and ponds are significant sources of carbon to the atmosphere due to
583 respiration of organic material of terrestrial origin (Pilla et al., 2022). Growing inputs of plant
584 detritus into lakes and rivers lead to browning (Blanchet et al., 2022), and increased frequency
585 and severity of wildfires (Pausas & Keeley, 2021) are two symptoms of recent global climate
586 change and human activities. Our results indicate that these two forces may interact in ways that
587 affect the capacity of aquatic systems to store, process and emit carbon. Accurate forecasts of
588 ongoing climate change require integrative models that incorporate feedbacks within and
589 between aquatic and terrestrial ecosystems and consideration of how changing ignition patterns
590 and wildfires will modify the global carbon cycle.
591

592 **Acknowledgements**
593 We thank Tobias Bautista, Kirby Inocente, Tristie Le, Ariana Brisco-Schoefield, Keyshawn
594 Ford, Wenbo Ding, Ryan Koch, and Dr. Elisabet Perez Coronel for their assistance in data
595 collection and processing, Dr. Eric Schmelz for logistical support, and Emily Schick and the
596 University of California-Davis Stable Isotope Facility for isotope and greenhouse gas analyses.

This project was funded by support from the National Science Foundation (award number 2018058).

Conflict of Interest Statement

The authors declare no conflicts of interest.

Data accessibility

All data and scripts are available at Github (http://www.github.com/cbwall/Pyromania) and are archived at Zenodo (xxx – will update following peer review).

Figure legends

Figure 1. DOC concentration across time in treatments receiving burned and unburned plant material at the start of the experiment and four sampling periods after plant material added. Lines represent linear regression and GAMs fit to data with 95% confidence intervals. Lines represent best-fit generalized additive models (GAMs) with treatment-level 95% confidence intervals. Black lines with gray confidence intervals indicate global smoothers across all data points; solid (*burned*) and dotted (*unburned*) colored lines indicate factor-smooths that vary between treatments.

Figure 2. (**A**) Net ecosystem productivity (NPP) and (**B**) respiration (R) in treatments receiving burned and unburned plant material across four sampling periods. Lines represent best-fit generalized additive models (GAMs) with treatment-level 95% confidence intervals. Black lines with gray confidence intervals indicate global smoothers across all data points; solid (*burned*)

and dotted (*unburned*) black lines together represent treatment-level intercepts with global smoothers; colored lines indicate factor-smooths that vary between treatments.

Figure 3. Trophic transfer as the % sage-derived ^{15}N from a two-source mixing model as a metric for plant-based subsidies in treatments receiving burned and unburned plant material at Days-10 and 31. Lines represent best-fit generalized additive models (GAMs) with treatment-level 95% confidence intervals.

Figure 4. Greenhouse gas concentration for (**A**) carbon dioxide (CO_2) and (**B**) methane (CH_4) at the beginning of the study before plant material was added (Day-0) and across three experimental time points. Lines represent best-fit generalized additive models (GAMs) with treatment-level 95% confidence intervals. Black lines with gray confidence intervals indicate global smoothers across all data points; solid (*burned*) and dotted (*unburned*) black lines together represent treatment-level intercepts with global smoothers; colored lines indicate factor-smooths that vary between treatments.

References

Ball, G., Regier, P., González-Pinzón, R., Reale, J., & Van Horn, D. (2021). Wildfires increasingly impact western US fluvial networks. *Nature Communications*, *12*(1), 2484. https://doi.org/10.1038/s41467-021-22747-3

Barneche, D. R., Hulatt, C. J., Dossena, M., Padfield, D., Woodward, G., Trimmer, M., & Yvon-Durocher, G. (2021). Warming impairs trophic transfer efficiency in a long-term field experiment. *Nature*, *592*(7852), 76–79. https://doi.org/10.1038/s41586-021-03352-2

Bixby, R. J., Cooper, S. D., Gresswell, R. E., Brown, L. E., Dahm, C. N., & Dwire, K. A. (2015). Fire effects on aquatic ecosystems: an assessment of the current state of the science. *Freshwater Science* , *34*(4), 1340–1350. https://doi.org/10.1086/684073

Bladon, K. D., Silins, U., Wagner, M. J., Stone, M., Emelko, M. B., Mendoza, C. A., Devito, K. J., & Boon, S. (2008). Wildfire impacts on nitrogen concentration and production from headwater streams in southern Alberta's Rocky Mountains. *Canadian Journal of Forest Research. Journal Canadien de La Recherche Forestiere*, *38*(9), 2359–2371. https://doi.org/10.1139/x08-071

Blanchet, C. C., Arzel, C., Davranche, A., Kahilainen, K. K., Secondi, J., Taipale, S., Lindberg, H., Loehr, J., Manninen-Johansen, S., Sundell, J., Maanan, M., & Nummi, P. (2022). Ecology and extent of freshwater browning - What we know and what should be studied next in the context of global change. *The Science of the Total Environment*, *812*, 152420. https://doi.org/10.1016/j.scitotenv.2021.152420

Bowman, D. M. J. S., Balch, J. K., Artaxo, P., Bond, W. J., Carlson, J. M., Cochrane, M. A., D'Antonio, C. M., Defries, R. S., Doyle, J. C., Harrison, S. P., Johnston, F. H., Keeley, J. E., Krawchuk, M. A., Kull, C. A., Marston, J. B., Moritz, M. A., Prentice, I. C., Roos, C. I.,

Scott, A. C., … Pyne, S. J. (2009). Fire in the Earth system. *Science*, *324*(5926), 481–484. https://doi.org/10.1126/science.1163886

Brett, M. T., Kainz, M. J., Taipale, S. J., & Seshan, H. (2009). Phytoplankton, not allochthonous carbon, sustains herbivorous zooplankton production. *Proceedings of the National Academy of Sciences of the United States of America*, *106*(50), 21197–21201. https://doi.org/10.1073/pnas.0904129106

Butler, O. M., Elser, J. J., Lewis, T., Maunsell, S. C., Rezaei Rashti, M., & Chen, C. (2020). The multi-element stoichiometry of wet eucalypt forest is transformed by recent, frequent fire. *Plant and Soil*, *447*(1), 447–461. https://doi.org/10.1007/s11104-019-04397-z

Butler, O. M., Lewis, T., Maunsell, S. C., Rezaei Rashti, M., Elser, J. J., Mackey, B., & Chen, C. (2021). The stoichiometric signature of high-frequency fire in forest floor food webs. *Ecological Monographs*. https://doi.org/10.1002/ecm.1477

Carignan, R., D'Arcy, P., & Lamontagne, S. (2000). Comparative impacts of fire and forest harvesting on water quality in Boreal Shield lakes. *Canadian Journal of Fisheries and Aquatic Sciences. Journal Canadien Des Sciences Halieutiques et Aquatiques*, *57*(S2), 105–117.

Cole, J. J., Carpenter, S. R., Kitchell, J. F., & Pace, M. L. (2002). Pathways of organic carbon utilization in small lakes: Results from a whole-lake ^{13}C addition and coupled model. *Limnology and Oceanography*, *47*(6), 1664–1675. https://doi.org/10.4319/lo.2002.47.6.1664

Cole, J. J., Carpenter, S. R., Kitchell, J., Pace, M. L., Solomon, C. T., & Weidel, B. (2011). Strong evidence for terrestrial support of zooplankton in small lakes based on stable isotopes of carbon, nitrogen, and hydrogen. *Proceedings of the National Academy of Sciences of the United States of America*, *108*(5), 1975–1980. https://doi.org/10.1073/pnas.1012807108

689 Cole, J. J., Carpenter, S. R., Pace, M. L., Van de Bogert, M. C., Kitchell, J. L., & Hodgson, J. R.
690 (2006). Differential support of lake food webs by three types of terrestrial organic carbon.
691 *Ecology Letters*, *9*(5), 558–568. https://doi.org/10.1111/j.1461-0248.2006.00898.x
692 Cole, J. J., Findlay, S., & Pace, M. L. (1988). Bacterial production in fresh and saltwater
693 ecosystems: a cross-system overview. *Marine Ecology Progress Series*.
694 https://doi.org/10.3354/meps043001
695 Coretta, S., van Rij, J., & Wieling, M. (2022). Tidymv: tidy model visualisation for generalised
696 additive models. *R Package Version*. https://cran.r-
697 project.org/web/packages/tidymv/index.html
698 Dahm, C. N., Candelaria-Ley, R. I., Reale, C. S., Reale, J. K., & Van Horn, D. J. (2015).
699 Extreme water quality degradation following a catastrophic forest fire. *Freshwater Biology*,
700 *60*(12), 2584–2599. https://doi.org/10.1111/fwb.12548
701 Diemer, L. A., McDowell, W. H., Wymore, A. S., & Prokushkin, A. S. (2015). Nutrient uptake
702 along a fire gradient in boreal streams of Central Siberia. *Freshwater Science* , *34*(4), 1443–
703 1456. https://doi.org/10.1086/683481
704 Fei, S., Morin, R. S., Oswalt, C. M., & Liebhold, A. M. (2019). Biomass losses resulting from
705 insect and disease invasions in US forests. *Proceedings of the National Academy of Sciences*
706 *of the United States of America*, *116*(35), 17371–17376.
707 https://doi.org/10.1073/pnas.1820601116
708 Fox, J., Weisberg, S., Price, B., Adler, D., Bates, D., Baud-Bovy, G., Bolker, B., & Others.
709 (2019). *car: Companion to Applied Regression. R package version 3.0-2*. Sage.
710 https://socialsciences.mcmaster.ca/jfox/Books/Companion/
711 Hampton, T. B., Lin, S., & Basu, N. B. (2022). Forest fire effects on stream water quality at

712 continental scales: a meta-analysis. *Environmental Research Letters: ERL [Web Site]*, *17*(6),
713 064003. https://doi.org/10.1088/1748-9326/ac6a6c
714 Hättenschwiler, S., & Vitousek, P. M. (2000). The role of polyphenols in terrestrial ecosystem
715 nutrient cycling. *Trends in Ecology & Evolution*, *15*(6), 238–243.
716 https://doi.org/10.1016/s0169-5347(00)01861-9
717 Hicke, J. A., Allen, C. D., Desai, A. R., Dietze, M. C., Hall, R. J., Ted Hogg, E. H., Kashian, D.
718 M., Moore, D., Raffa, K. F., Sturrock, R. N., & Vogelmann, J. (2012). Effects of biotic
719 disturbances on forest carbon cycling in the United States and Canada. *Global Change*
720 *Biology*, *18*(1), 7–34. https://doi.org/10.1111/j.1365-2486.2011.02543.x
721 Isidorova, A., Bravo, A. G., Riise, G., Bouchet, S., Björn, E., & Sobek, S. (2016). The effect of
722 lake browning and respiration mode on the burial and fate of carbon and mercury in the
723 sediment of two boreal lakes. *Journal of Geophysical Research. Biogeosciences*, *121*(1),
724 233–245. https://doi.org/10.1002/2015jg003086
725 Jones, M. W., Abatzoglou, J. T., Veraverbeke, S., Andela, N., Lasslop, G., Forkel, M., Smith, A.
726 J. P., Burton, C., Betts, R. A., van der Werf, G. R., Sitch, S., Canadell, J. G., Santín, C.,
727 Kolden, C., Doerr, S. H., & Le Quéré, C. (2022). Global and regional trends and drivers of
728 fire under climate change. *Reviews of Geophysics* , *60*(3).
729 https://doi.org/10.1029/2020rg000726
730 Jones, R. I. (1992). The influence of humic substances on lacustrine planktonic food chains.
731 *Hydrobiologia*, *229*(1), 73–91. https://doi.org/10.1007/bf00006992
732 Jones, S. E., & Lennon, J. T. (2015). A test of the subsidy–stability hypothesis: the effects of
733 terrestrial carbon in aquatic ecosystems. *Ecology*, *96*(6), 1550–1560.
734 https://doi.org/10.1890/14-1783.1

735 Karpowicz, M., Feniova, I., Gladyshev, M. I., Ejsmont-Karabin, J., Górniak, A., Sushchik, N. N.,
736 Anishchenko, O. V., & Dzialowski, A. R. (2021). Transfer efficiency of carbon, nutrients,
737 and polyunsaturated fatty acids in planktonic food webs under different environmental
738 conditions. *Ecology and Evolution*, *11*(12), 8201–8214. https://doi.org/10.1002/ece3.7651
739 Kelly, P. T., Solomon, C. T., Weidel, B. C., & Jones, S. E. (2014). Terrestrial carbon is a
740 resource, but not a subsidy, for lake zooplankton. *Ecology*, *95*(5), 1236–1242.
741 https://doi.org/10.1890/13-1586.1
742 Kokic, J., Wallin, M. B., Chmiel, H. E., Denfeld, B. A., & Sobek, S. (2015). Carbon dioxide
743 evasion from headwater systems strongly contributes to the total export of carbon from a
744 small boreal lake catchment. *Journal of Geophysical Research. Biogeosciences*, *120*(1), 13–
745 28. https://doi.org/10.1002/2014jg002706
746 Koschorreck, M., Prairie, Y. T., Kim, J., & Marcé, R. (2021). Technical note: CO_2 is not like
747 CH_4 – limits of and corrections to the headspace method to analyse pCO_2 in fresh water.
748 *Biogeosciences* , *18*(5), 1619–1627. https://doi.org/10.5194/bg-18-1619-2021
749 Larsen, I. J., MacDonald, L. H., Brown, E., Rough, D., Welsh, M. J., Pietraszek, J. H., Libohova,
750 Z., Dios Benavides-Solorio, J., & Schaffrath, K. (2009). Causes of post-fire runoff and
751 erosion: water repellency, cover, or soil sealing? *Soil Science Society of America Journal.*
752 *Soil Science Society of America*, *73*(4), 1393–1407. https://doi.org/10.2136/sssaj2007.0432
753 Lasslop, G., Coppola, A. I., Voulgarakis, A., Yue, C., & Veraverbeke, S. (2019). Influence of
754 fire on the carbon cycle and climate. *Current Climate Change Reports*, *5*(2), 112–123.
755 https://doi.org/10.1007/s40641-019-00128-9
756 Lennon, J. T. (2004). Experimental evidence that terrestrial carbon subsidies increase CO_2 flux
757 from lake ecosystems. *Oecologia*, *138*(4), 584–591. http://www.jstor.org/stable/40005540

758 Lennon, J. T., & Pfaff, L. E. (2005). Source and supply of terrestrial organic matter affects
759 aquatic microbial metabolism. *Aquatic Microbial Ecology: International Journal*, *39*, 107–
760 119. https://doi.org/10.3354/ame039107
761 Lewis, J., Rhodes, J. J., & Bradley, C. (2019). Turbidity responses from timber harvesting,
762 wildfire, and post-fire logging in the Battle Creek Watershed, Northern California.
763 *Environmental Management*, *63*(3), 416–432. https://doi.org/10.1007/s00267-018-1036-3
764 Liu, D., Zhou, C., Keesing, J. K., Serrano, O., Werner, A., Fang, Y., Chen, Y., Masque, P.,
765 Kinloch, J., Sadekov, A., & Du, Y. (2022). Wildfires enhance phytoplankton production in
766 tropical oceans. *Nature Communications*, *13*(1), 1348. https://doi.org/10.1038/s41467-022-
767 29013-0
768 Liu, Y., Stanturf, J., & Goodrick, S. (2010). Trends in global wildfire potential in a changing
769 climate. *Forest Ecology and Management*, *259*(4), 685–697.
770 https://doi.org/10.1016/j.foreco.2009.09.002
771 Liu, Z., Deng, Z., Davis, S. J., Giron, C., & Ciais, P. (2022). Monitoring global carbon emissions
772 in 2021. *Nature Reviews. Earth & Environment*, *3*(4), 217–219.
773 https://doi.org/10.1038/s43017-022-00285-w
774 McCullough, I. M., Cheruvelil, K. S., Lapierre, J.-F., Lottig, N. R., Moritz, M. A., Stachelek, J.,
775 & Soranno, P. A. (2019). Do lakes feel the burn? Ecological consequences of increasing
776 exposure of lakes to fire in the continental United States. *Global Change Biology*, *25*(9),
777 2841–2854. https://doi.org/10.1111/gcb.14732
778 McLauchlan, K. K., Higuera, P. E., Miesel, J., Rogers, B. M., Schweitzer, J., Shuman, J. K.,
779 Tepley, A. J., Varner, J. M., Veblen, T. T., Adalsteinsson, S. A., Balch, J. K., Baker, P.,
780 Batllori, E., Bigio, E., Brando, P., Cattau, M., Chipman, M. L., Coen, J., Crandall, R., …

781 Watts, A. C. (2020). Fire as a fundamental ecological process: Research advances and
782 frontiers. *The Journal of Ecology*, *108*(5), 2047–2069. https://doi.org/10.1111/1365-
783 2745.13403
784 Minshall, G. W., Brock, J. T., Andrews, D. A., & Robinson, C. T. (2001). Water quality,
785 substratum and biotic responses of five central Idaho (USA) streams during the first year
786 following the Mortar Creek fire. *International Journal of Wildland Fire*, *10*(2), 185.
787 https://doi.org/10.1071/wf01017
788 Natali, S. M., Holdren, J. P., Rogers, B. M., Treharne, R., Duffy, P. B., Pomerance, R., &
789 MacDonald, E. (2021). Permafrost carbon feedbacks threaten global climate goals.
790 *Proceedings of the National Academy of Sciences of the United States of America*, *118*(21).
791 https://doi.org/10.1073/pnas.2100163118
792 Obernosterer, I., & Benner, R. (2004). Competition between biological and photochemical
793 processes in the mineralization of dissolved organic carbon. *Limnology and Oceanography*,
794 *49*(1), 117–124. https://doi.org/10.4319/lo.2004.49.1.0117
795 Paul, M. J., LeDuc, S. D., Lassiter, M. G., Moorhead, L. C., Noyes, P. D., & Leibowitz, S. G.
796 (2022). Wildfire induces changes in receiving waters: A review with considerations for
797 water quality management. *Water Resources Research*, *58*(9).
798 https://doi.org/10.1029/2021wr030699
799 Pausas, J. G., & Keeley, J. E. (2021). Wildfires and global change. *Frontiers in Ecology and the*
800 *Environment*, *19*(7), 387–395. https://doi.org/10.1002/fee.2359
801 Pedersen, E. J., Miller, D. L., Simpson, G. L., & Ross, N. (2019). Hierarchical generalized
802 additive models in ecology: an introduction with mgcv. *PeerJ*, *7*, e6876.
803 https://doi.org/10.7717/peerj.6876

Pellegrini, A. F. A., Harden, J., Georgiou, K., Hemes, K. S., Malhotra, A., Nolan, C. J., & Jackson, R. B. (2021). Fire effects on the persistence of soil organic matter and long-term carbon storage. *Nature Geoscience*, *15*(1), 5–13. https://doi.org/10.1038/s41561-021-00867-1

Perez-Coronel, E., Hart, S. C., & Beman, J. M. (2021). Methane dynamics of high-elevation lakes in the Sierra Nevada California: the role of elevation, temperature, and inorganic nutrients. *Inland Waters*, *11*(3), 267–277. https://doi.org/10.1080/20442041.2021.1903287

Perez-Coronel, E., & Michael Beman, J. (2022). Multiple sources of aerobic methane production in aquatic ecosystems include bacterial photosynthesis. *Nature Communications*, *13*(1), 6454. https://doi.org/10.1038/s41467-022-34105-y

Pilla, R. M., Griffiths, N. A., Gu, L., Kao, S.-C., McManamay, R., Ricciuto, D. M., & Shi, X. (2022). Anthropogenically driven climate and landscape change effects on inland water carbon dynamics: What have we learned and where are we going? *Global Change Biology*, *28*(19), 5601–5629. https://doi.org/10.1111/gcb.16324

Post, D. M. (2002). Using stable isotopes to estimate trophic position: Models, methods, and assumptions. *Ecology*, *83*(3), 703. https://doi.org/10.2307/3071875

Ramberg, L., Lindholm, M., Hessen, D. O., Murray-Hudson, M., Bonyongo, C., Heinl, M., Masamba, W., VanderPost, C., & Wolski, P. (2010). Aquatic ecosystem responses to fire and flood size in the Okavango Delta: observations from the seasonal floodplains. *Wetlands Ecology and Management*, *18*(5), 587–595. https://doi.org/10.1007/s11273-010-9195-x

Rodríguez-Cardona, B. M., Coble, A. A., Wymore, A. S., Kolosov, R., Podgorski, D. C., Zito, P., Spencer, R. G. M., Prokushkin, A. S., & McDowell, W. H. (2020). Wildfires lead to decreased carbon and increased nitrogen concentrations in upland arctic streams. *Scientific*

Reports, *10*(1), 8722. https://doi.org/10.1038/s41598-020-65520-0

Rodríguez-Lozano, P., Rieradevall, M., Rau, M. A., & Prat, N. (2015). Long-term consequences of a wildfire for leaf-litter breakdown in a Mediterranean stream. *Freshwater Science* , *34*(4), 1482–1493. https://doi.org/10.1086/683432

Rust, A. J., Hogue, T. S., Saxe, S., & McCray, J. (2018). Post-fire water-quality response in the western United States. *International Journal of Wildland Fire*, *27*(3), 203–216. https://doi.org/10.1071/WF17115

Santos, F., Wymore, A. S., Jackson, B. K., Sullivan, S. M. P., McDowell, W. H., & Berhe, A. A. (2019). Fire severity, time since fire, and site-level characteristics influence streamwater chemistry at baseflow conditions in catchments of the Sierra Nevada, California, USA. *Fire Ecology*, *15*(1), 1–15. https://doi.org/10.1186/s42408-018-0022-8

Simpson, G. L. (2022). gratia: Graceful "ggplot"-based graphics and other functions for GAMs fitted using "mgcv." *R Package Version 0.7.3*. https://gavinsimpson.github.io/gratia/

Sobek, S., Algesten, G., Bergström, A.-K., Jansson, M., & Tranvik, L. J. (2003). The catchment and climate regulation of pCO_2 in boreal lakes. *Global Change Biology*, *9*(4), 630–641. https://doi.org/10.1046/j.1365-2486.2003.00619.x

Solomon, C. T., Jones, S. E., Weidel, B. C., Buffam, I., Fork, M. L., Karlsson, J., Larsen, S., Lennon, J. T., Read, J. S., Sadro, S., & Saros, J. E. (2015). Ecosystem consequences of changing inputs of terrestrial dissolved organic matter to lakes: current knowledge and future challenges. *Ecosystems* , *18*(3), 376–389. https://doi.org/10.1007/s10021-015-9848-y

Spencer, C. N., Gabel, K. O., & Hauer, F. R. (2003). Wildfire effects on stream food webs and nutrient dynamics in Glacier National Park, USA. *Forest Ecology and Management*, *178*(1), 141–153. https://doi.org/10.1016/S0378-1127(03)00058-6

Stetler, J. T., Knoll, L. B., Driscoll, C. T., & Rose, K. C. (2021). Lake browning generates a spatiotemporal mismatch between dissolved organic carbon and limiting nutrients. *Limnology and Oceanography Letters*, *6*(4), 182–191. https://doi.org/10.1002/lol2.10194

Tang, W., Llort, J., Weis, J., Perron, M. M. G., Basart, S., Li, Z., Sathyendranath, S., Jackson, T., Sanz Rodriguez, E., Proemse, B. C., Bowie, A. R., Schallenberg, C., Strutton, P. G., Matear, R., & Cassar, N. (2021). Widespread phytoplankton blooms triggered by 2019-2020 Australian wildfires. *Nature*, *597*(7876), 370–375. https://doi.org/10.1038/s41586-021-03805-8

Ward, N. D., Bianchi, T. S., Medeiros, P. M., Seidel, M., Richey, J. E., Keil, R. G., & Sawakuchi, H. O. (2017). Where carbon goes when water flows: carbon cycling across the aquatic continuum. *Frontiers in Marine Science*, *4*. https://doi.org/10.3389/fmars.2017.00007

Weiss, R. F. (1974). Carbon dioxide in water and seawater: the solubility of a non-ideal gas. *Marine Chemistry*, *2*(3), 203–215. https://doi.org/10.1016/0304-4203(74)90015-2

Whitney, J. E., Gido, K. B., Pilger, T. J., Propst, D. L., & Turner, T. F. (2015). Consecutive wildfires affect stream biota in cold- and warmwater dryland river networks. *Freshwater Science* , *34*(4), 1510–1526. https://doi.org/10.1086/683391

Wood, S. N. (2011). Fast stable restricted maximum likelihood and marginal likelihood estimation of semiparametric generalized linear models. *Journal of the Royal Statistical Society. Series B, Statistical Methodology*, *73*(1), 3–36. https://doi.org/10.1111/j.1467-9868.2010.00749.x

Yamamoto, S., Alcauskas, J. B., & Crozier, T. E. (1976). Solubility of methane in distilled water and seawater. *Journal of Chemical and Engineering Data*, *21*(1), 78–80.

https://doi.org/10.1021/je60068a029

Zheng, B., Ciais, P., Chevallier, F., Chuvieco, E., Chen, Y., & Yang, H. (2021). Increasing forest fire emissions despite the decline in global burned area. *Science Advances*, *7*(39), eabh2646. https://doi.org/10.1126/sciadv.abh2646

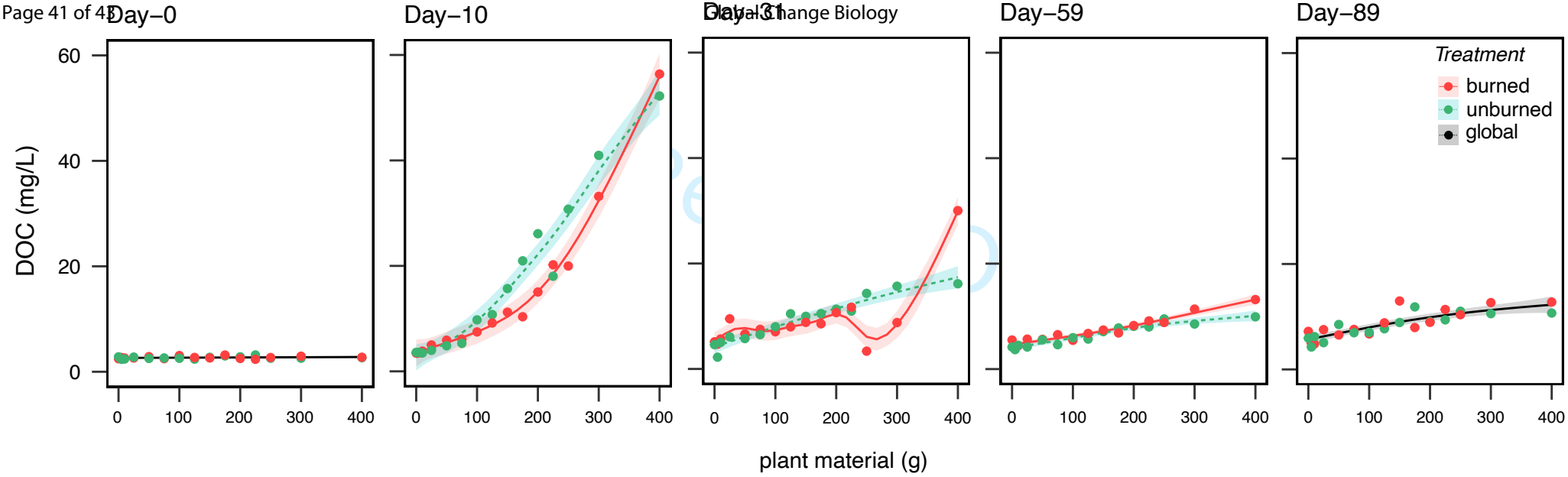
Day–0
Day–10
Day–31
Day–59
Day–89
DOC (mg/L)
0
20
40
60
0
100
200
300
400
plant material (g)
Treatment
burned
unburned
global

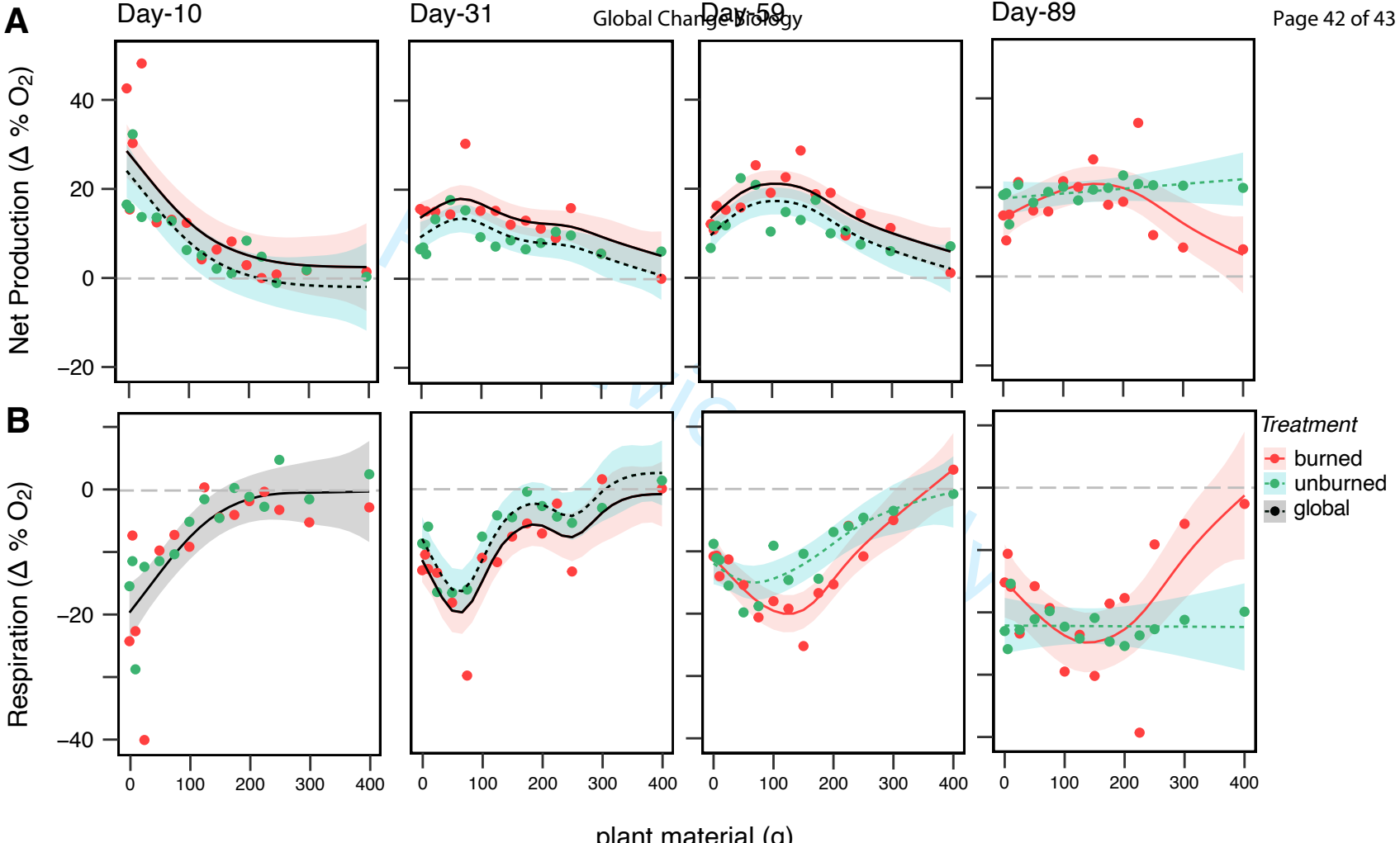
A
Day-10
Day-31
Day-59
Day-89
Net Production (Δ % O2)
40
20
0
−20
B
Respiration (Δ % O2)
0
−20
−40
0
100
200
300
400
plant material (g)
Treatment
burned
unburned
global

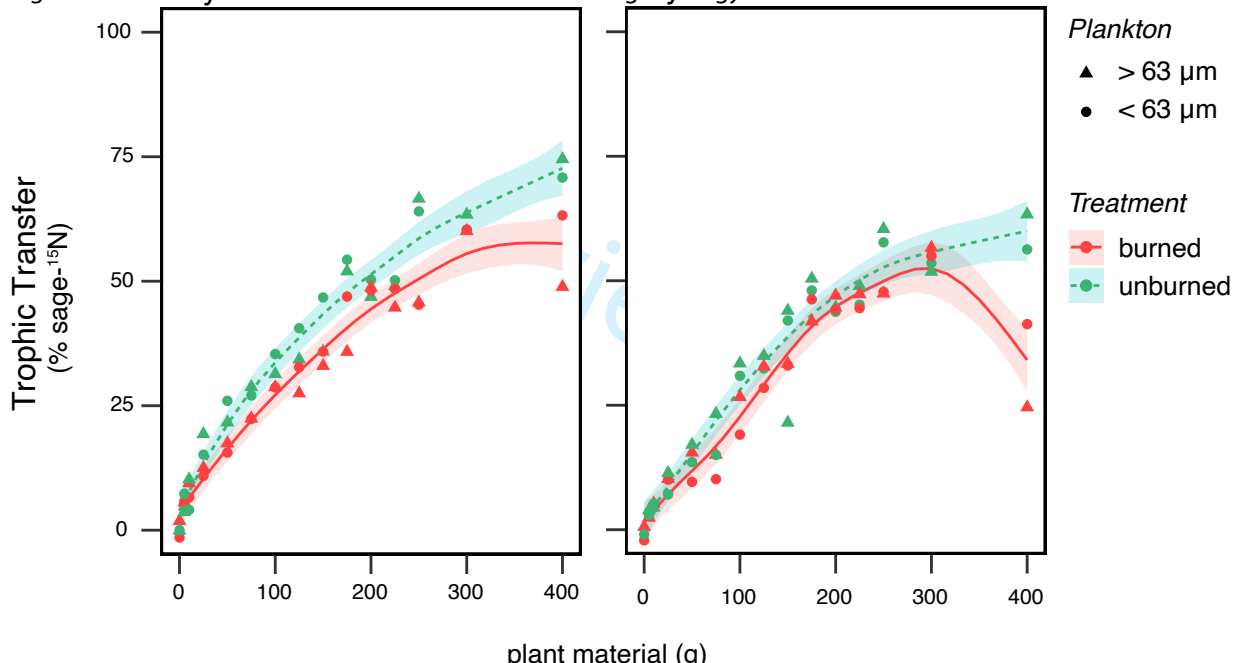
Day-10
Day-31
Trophic Transfer
(% sage-15N)
plant material (g)
0
25
50
75
100
0
100
200
300
400
Plankton
> 63 µm
< 63 µm
Treatment
burned
unburned

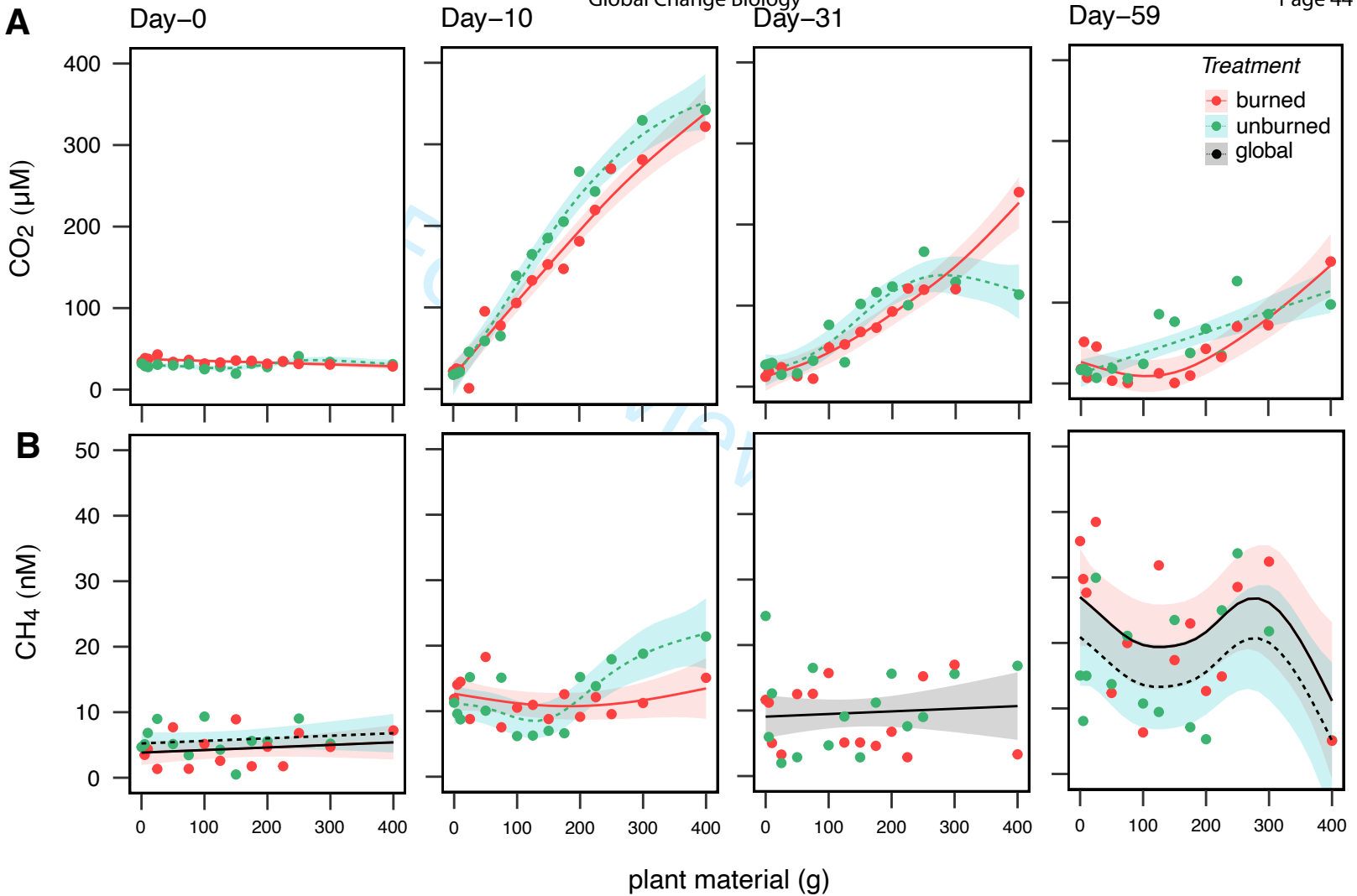
A
Day–0
Day–10
Day–31
Day–59
CO2 (μM)
400
300
200
100
0
Treatment
burned
unburned
global
B
CH4 (nM)
50
40
30
20
10
0
0
100
200
300
400
plant material (g)

Supplemental Materials for

Fire transforms effects of terrestrial subsidies on aquatic ecosystem structure and function

Christopher B. Wall, Cody J. Spiegel, Evelyn Diaz, Cindy Tran, Alexia Fabiani, Taryn Broe, Elisabet Perez-Coronel, Sara Jackrel, Natalie Mladenov, Ceila C. Symons, Jonathan B. Shurin

Corresponding author: Christopher B. Wall
Email: cbwall@ucsd.edu

This PDF file includes:

Supporting Text

Supplemental Results

Dissolved oxygen percent

Dissolved oxygen (DO as % O_2) measurements showed consistent patterns among replicate dawn measurements (separated by 24 h) in each time point (Fig. S6), although % O_2 showed considerable change over time. At Day-10, dawn and dusk % O_2 was consistently < 50 % in tanks receiving more than 100 g of plant material, with treatments > 200 g plant material showing hypoxic conditions (< 10 % O_2). Significant non-linear relationships between % O_2 and plant biomass were observed in all time points, with treatment-specific intercepts for a global smoother at Day-10 and significant non-linear relationships that varied by treatment for dawn-and-dusk measurements at Days-31 and 59 (*SI Appendix*, Tables S5 and S6). Measurements on Days-31 and 59 also showed significantly higher % O_2 in mid-range burned tanks (100-200g) compared to unburned, however, % O_2 was consistently lower in burned treatments at 400 g compared to unburned tanks (*SI Appendix*, Fig. S7). By Day-89, treatment effects were minimal although % O_2 remained higher in tanks receiving less plant materials (*SI Appendix*, Fig. S6).

Isotope labeling

Nitrogen isotope labeling (^{15}N) substantially increased the $\delta^{15}N$ isotope values of pooled burned-and-unburned sage leaf materials (mean ± SD; 296 ± 53 ‰) relative to willow (13 ± 0.3 ‰) (p<0.001) (Fig. S9, Table S9A). Burning treatment did not affect leaf $\delta^{15}N$ values for sage (p=0.423) or willow (p=0.485). C:N values were higher in burned relative to unburned sage (p=0.001), driven by higher C:N values (~ 70) in sage subjected to longer fire treatment (i.e., very-burned sage), but equivalent between burned and

unburned willow (p=0.061) (*SI Appendix*, Fig. S9 and Table S9A). $\delta^{15}N$ values did not differ between burned and unburned sage (p=0.423) or willow (p=0.485). Using pooled burned and unburned leaves, sage had C:N values slightly higher than willow (mean 49 and 47) (p=0.014) (*SI Appendix*, Fig. S9B). Plankton $\delta^{15}N$ values were slightly lower than those in the plankton (11 vs. 13 ‰) (p=0.001), and plankton C:N was significantly lower than willow (mean 5.8) (p<0.001) (*SI Appendix*, Fig. S9B and Table S9A).

Plankton $\delta^{15}N$ was used in isotope mixing models to determine the percent of sage-^{15}N incorporated into plankton biomass. Raw $\delta^{15}N$ values are reported in (*SI Appendix*, Fig. S9C, D). GAM models fit to raw $\delta^{15}N$ values can be found in (*SI Appendix*, Table S11).

The positive relationship between plankton nitrogen and carbon concentrations was similar among burned and unburned treatments (*SI Appendix*, Fig. S11) that did not differ across time or among plankton size fractions. Plankton C:N ratios showed significant nonlinearity across the plant-biomass gradient at Day-10 and Day-31 (p≤0.038) (*SI Appendix*, Table S11), with burned treatment plankton C:N being lower in mid-range tanks (100-150 g) at Day-10 and higher in high plat-biomass treatments (400 g) at Day-10 and Day-31 (*SI Appendix*, Fig. S12).

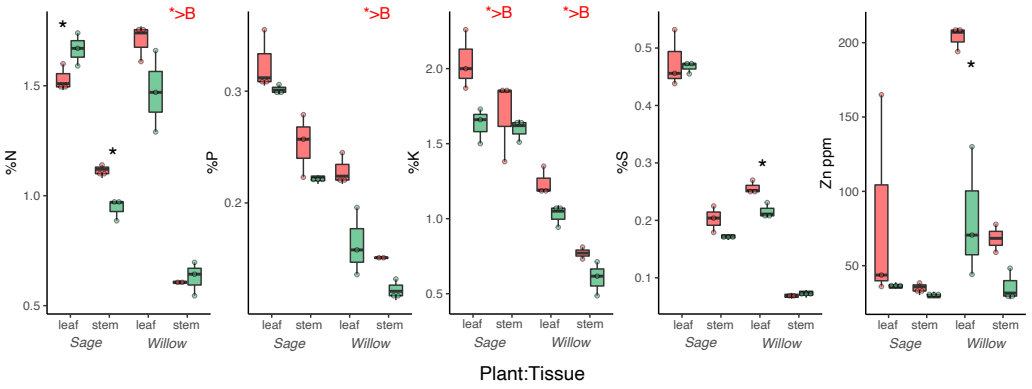

Figure S1. Elemental analysis of burned and unburned plant material (leaves and stem) from sage and willow prior to being added to experimental treatments. Significant post-hoc comparisons (p<0.05) of burned effects within a Plant:Tissue type are shown with *black asterisks*. *Red asterisks* indicate significant overall treatment effects and the direction of these effects for either sage or willow in the absence of interactions. Box plots depict the median (bold center line), first and third quartiles (lower and upper bounds), whiskers (1.5x the distance between first and third quartiles).

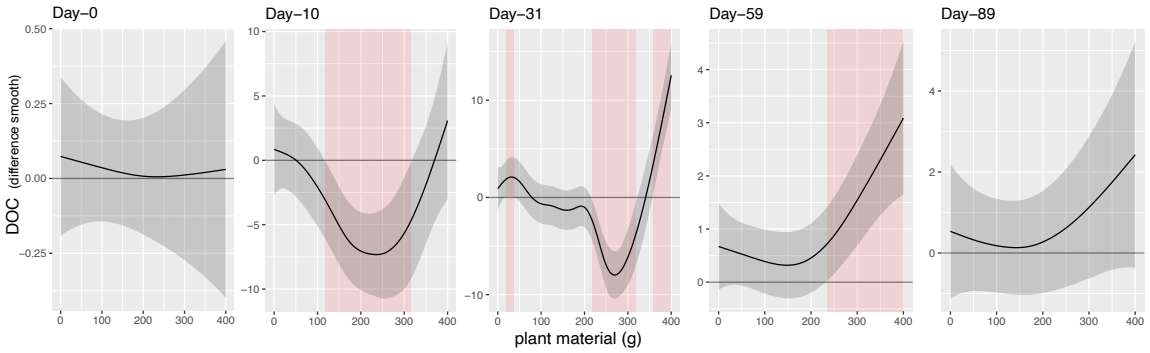

Figure S2. Model effects from GAMs with differences between smoothers for DOC concentration across time in treatments receiving burned and unburned plant material. Shaded regions are the confidence interval for 'the difference smooth,' which is the difference between burned and unburned treatment smoothers. Significant differences between treatment-level smoothers are noted in regions that do not include zero ± model confidence intervals and are shaded in pink.

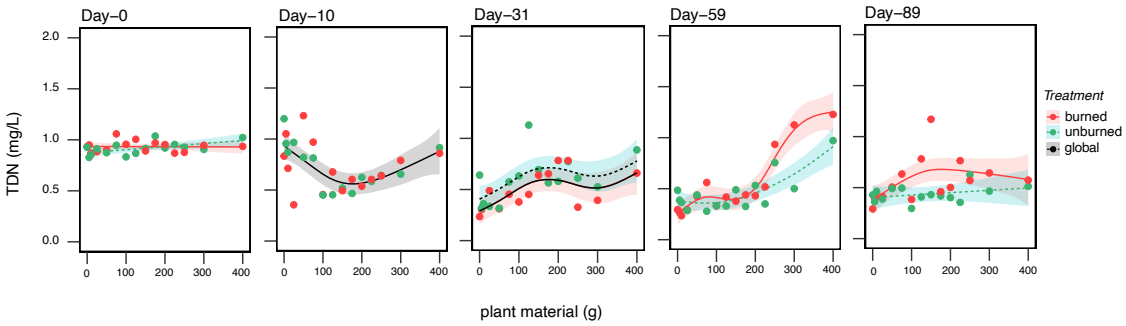

Figure S3. Total dissolved nitrogen (TDN) concentration across time in treatments receiving burned and unburned plant material. Lines represent best-fit generalized additive models (GAMs) with treatment-level 95% confidence intervals. Black lines with gray confidence intervals indicate global smoothers across all data points; solid (*burned*) and dotted (*unburned*) black lines together represent treatment-level intercepts with global smoothers; colored lines indicate factor-smooths that vary between treatments.

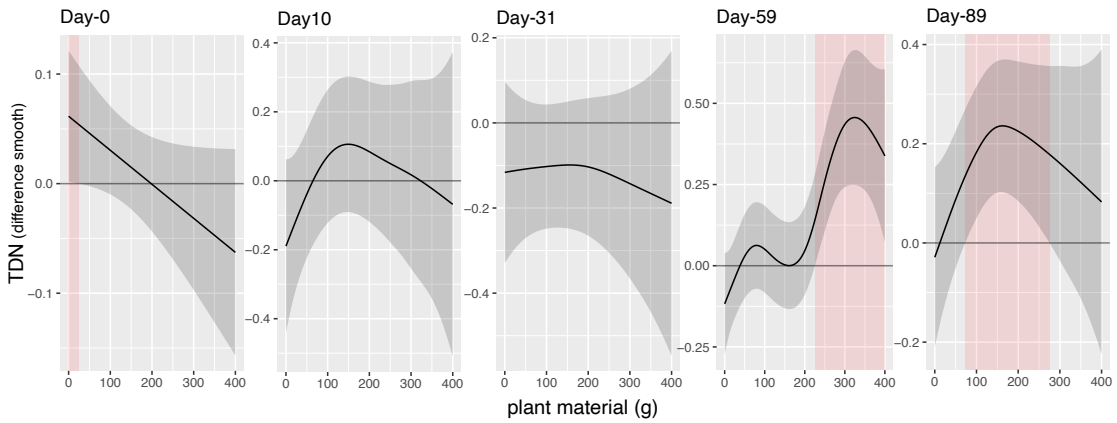

Figure S4. Model effects from GAMs with differences between smoothers for TN across time in treatments receiving burned and unburned plant material. Shaded regions are the confidence interval for 'the difference smooth,' which is the difference between burned and unburned treatment smoothers. Significant differences between treatment-level smoothers are noted in regions that do not include zero ± model confidence intervals and are shaded in pink.

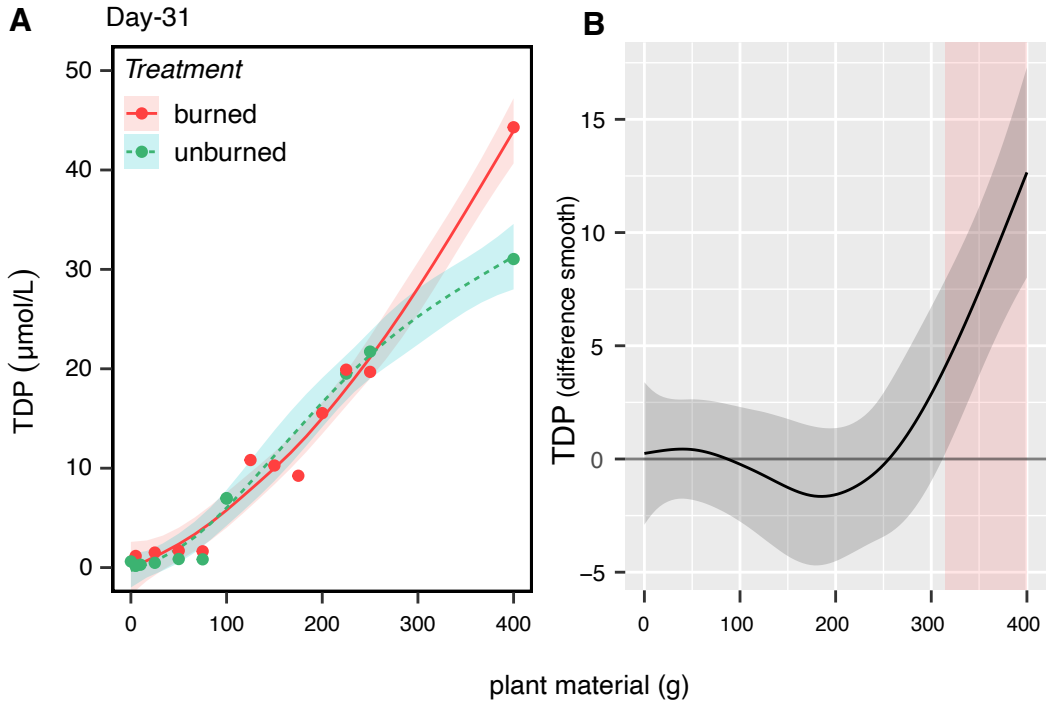

Figure S5. (A) Total phosphorus concentration in water from burned and unburned treatments at Day-31, and **(B)** the difference between burned and unburned treatment smoothers. Lines in *A* represent best-fit generalized additive models (GAMs) with treatment-level 95% confidence intervals. Lines in *B* represent differences between treatment-level smoothers, where significant differences (shaded in pink) are noted in regions that do not include zero ± model confidence intervals.

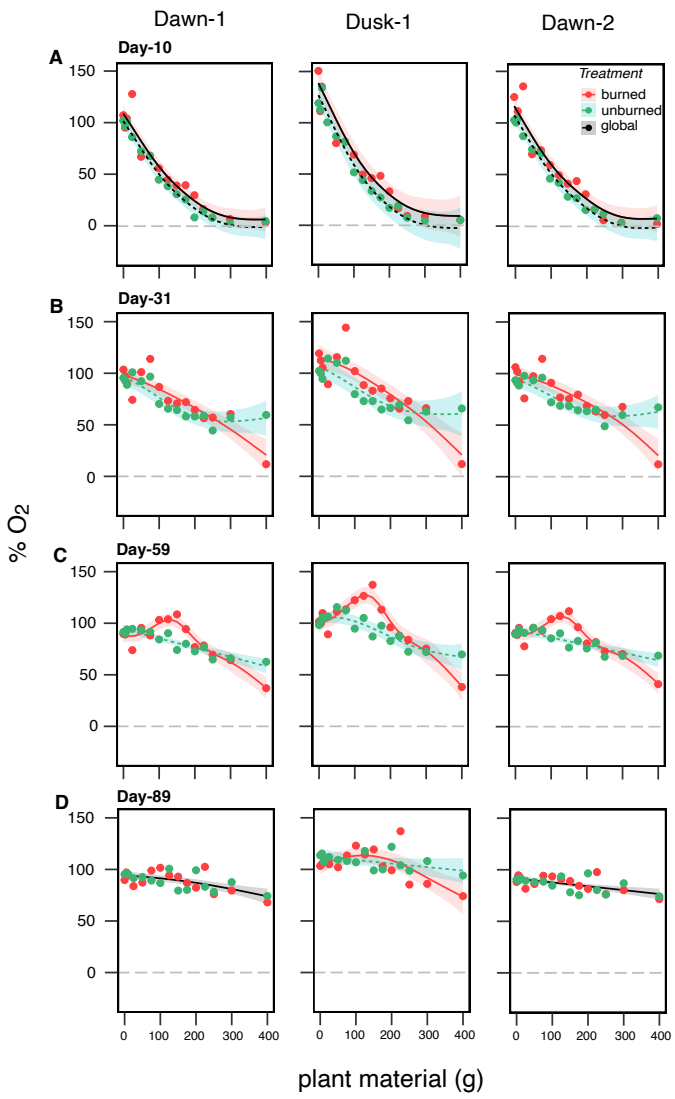

Figure S6. (A-D) Changes in dissolved oxygen concentration (%) at dawn and dusk across the four experimental period. Data here were used to calculate net ecosystem production and respiration. Lines represent best-fit generalized additive models (GAMs) with treatment-level 95% confidence intervals. Black lines with gray confidence intervals indicate global smoothers across all data points; solid (*burned*) and dotted (*unburned*) black lines together represent treatment-level intercepts with global smoothers; colored lines indicate factor-smooths that vary between treatments.

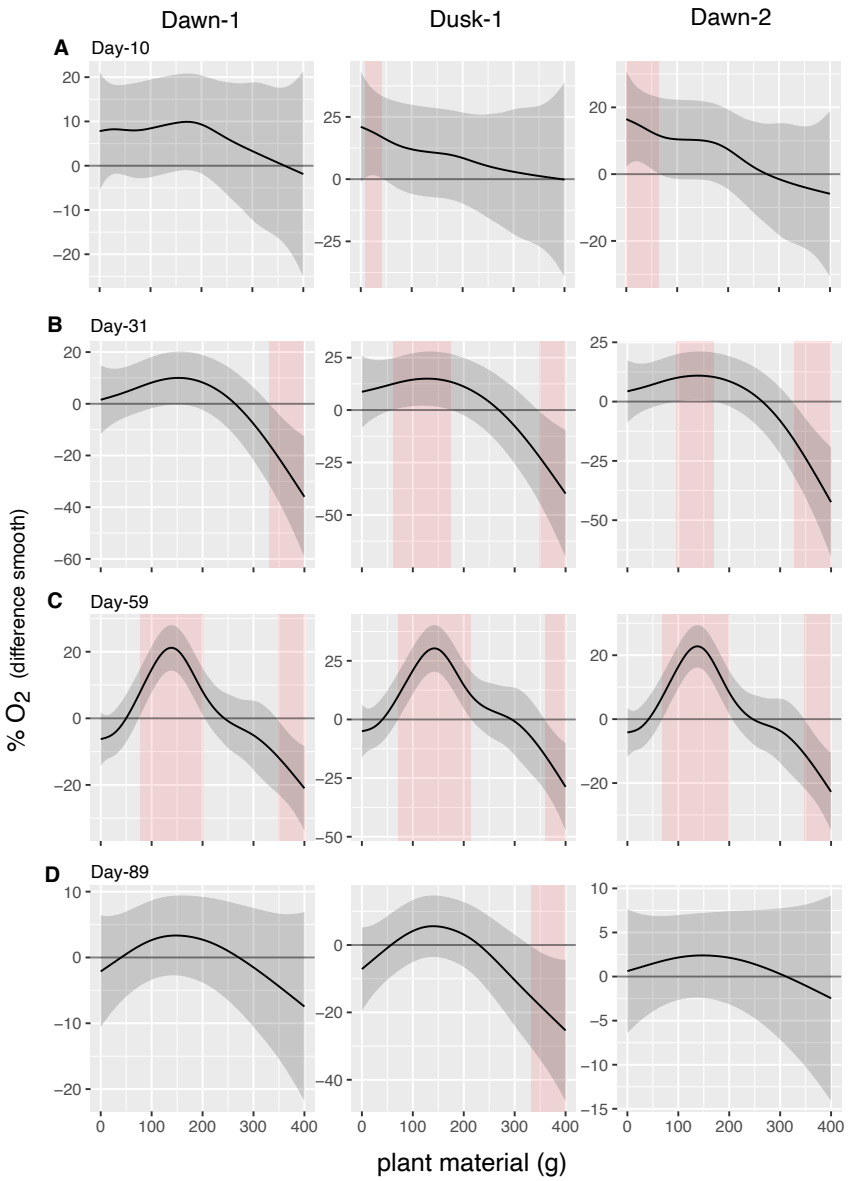

Figure S7. (**A-D**) Model effects from GAMs with differences between smoothers for oxygen concentration (% O_2) across four experimental time points in treatments receiving burned and unburned plant material. Shaded regions are the confidence interval for 'the difference smooth,' which is the difference between burned and unburned treatment smoothers. Significant differences between treatment-level

smoothers are noted in regions that do not include zero ± model confidence intervals and are shaded in pink.

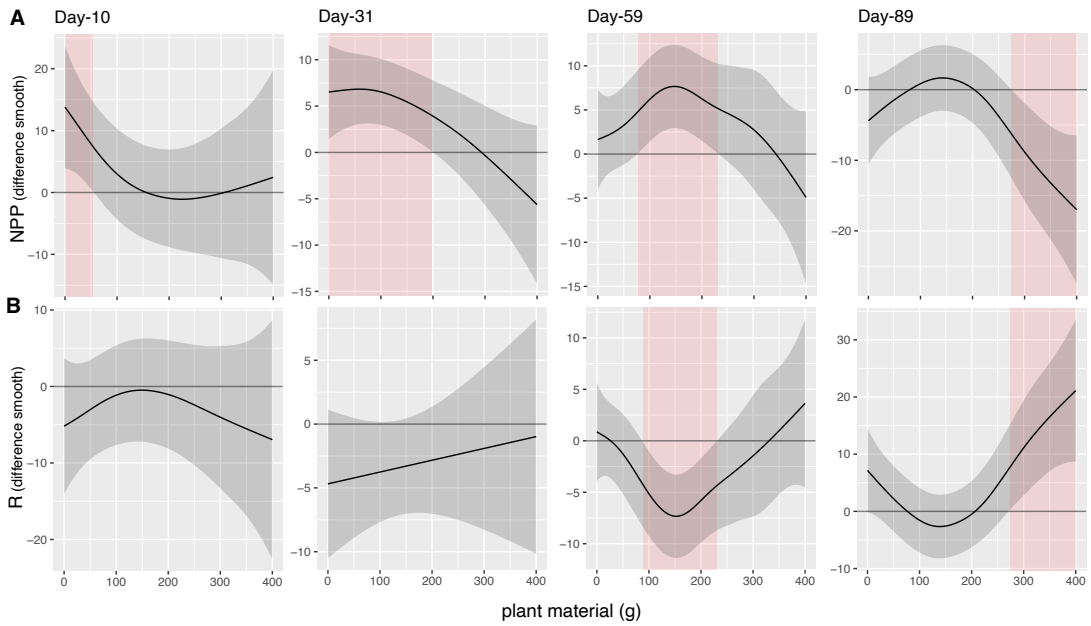

Figure S8. Model effects from GAMs with differences between smoothers for (**A**) net primary production (NPP) and (**B**) respiration (R) across time in treatments receiving burned and unburned plant material. Shaded regions are the confidence interval for 'the difference smooth,' which is the difference between burned and unburned treatment smoothers. Significant differences between treatment-level smoothers are noted in regions that do not include zero ± model confidence intervals and are shaded in pink.

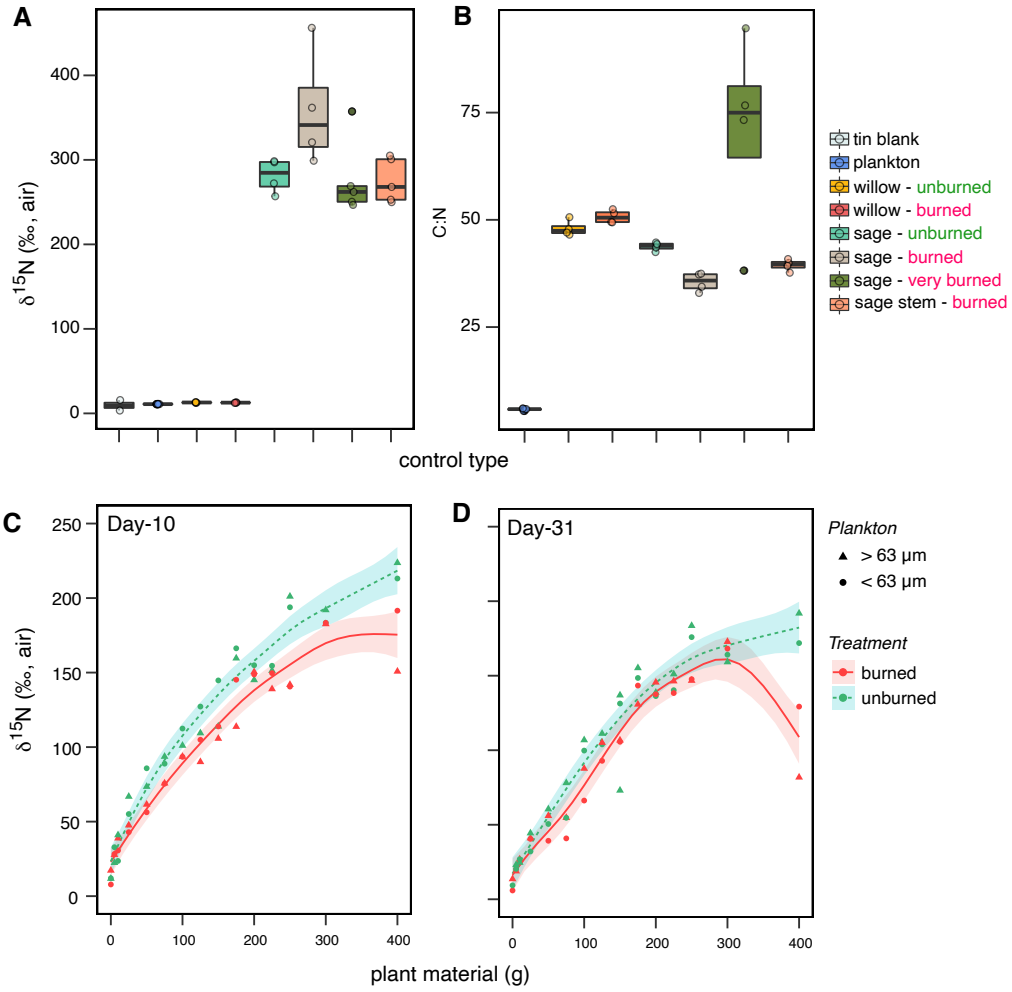

Figure S9. (A) Nitrogen isotope values and **(B)** C:N ratio for experimental controls (tin blanks), stock plankton, and burned or unburned plant material (willow, sage). **(C, D)** Nitrogen isotope values of plankton fractions in burned and unburned treatments at Day-10 (Time-1) and Day-31 (Time-2). Lines in the bottom panel represent GAMs fit to data with 95% confidence intervals. Box plots depict the median (bold center line), first and third quartiles (lower and upper bounds), whiskers (1.5x the distance between first and third quartiles), and outliers (black circles).

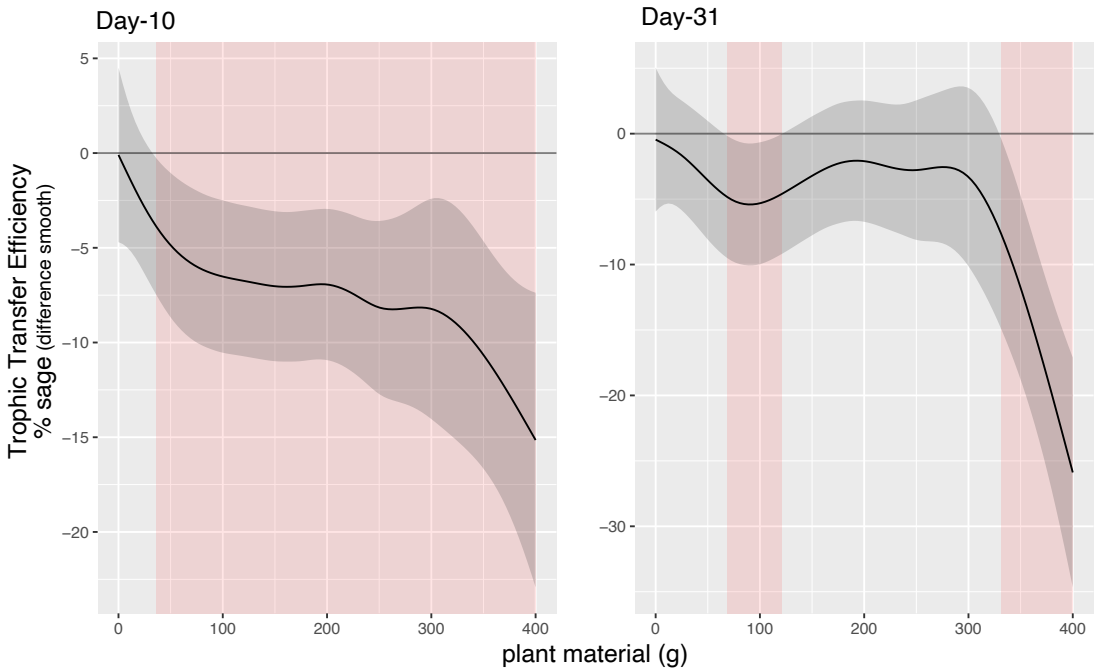

Figure S10. Model effects from GAMs with differences between smoothers for % sage-derived ^{15}N at Day-10 and Day-31 in tanks receiving burned and unburned plant material. Significant differences between treatment-level smoothers are noted in regions that do not include zero ± model confidence intervals and are shaded in pink.

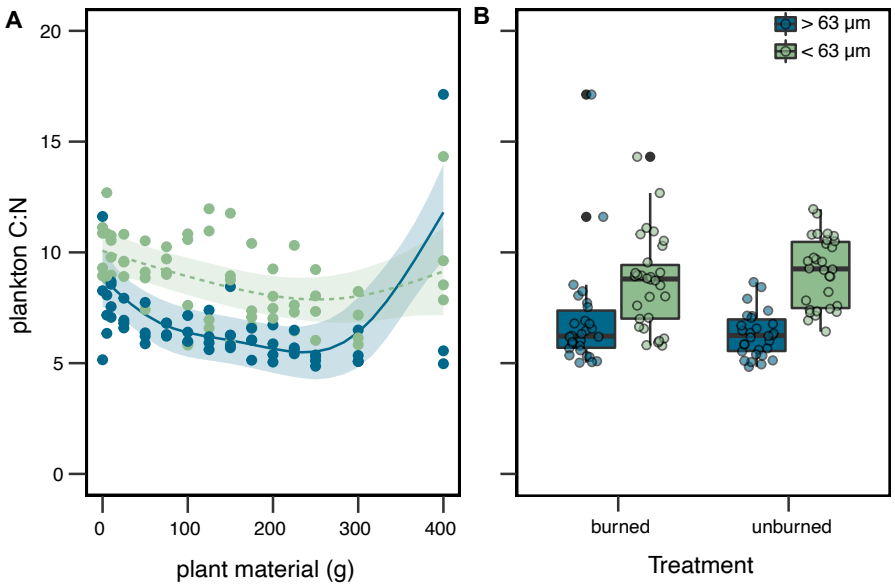

Figure S11. (A) Plankton C:N along the plant material gradient pooled across days (10 and 31) and treatments (burned and unburned), and **(B)** plankton C:N in treatment tanks receiving burned and unburned plant material. Lines represent GAMs (*top*) with treatment-level 95% confidence intervals. Box plots depict the median (bold center line), first and third quartiles (lower and upper bounds), whiskers (1.5x the distance between first and third quartiles), and outliers (black circles).

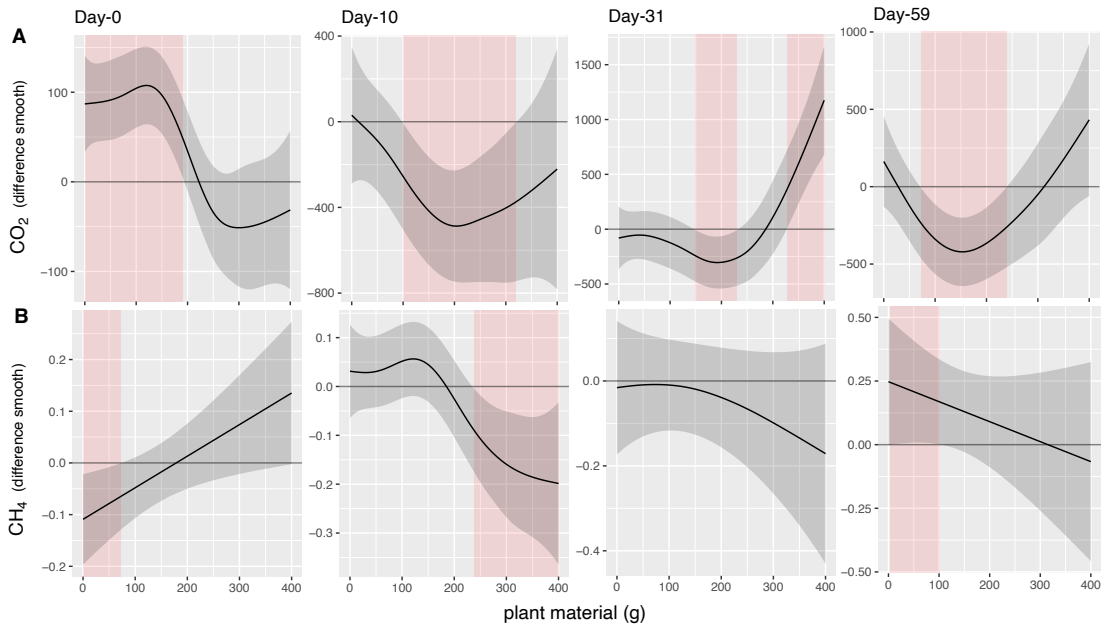

Figure S12. Model effects from GAMs with differences between smoothers for greenhouse gasses **(A)** carbon dioxide (CO_2) and **(B)** methane (CH_4) in tanks receiving burned and unburned plant material at the beginning of the experiment and during three experimental time points. Significant differences between treatment-level smoothers are noted in regions that do not include zero ± model confidence intervals and are shaded in pink.

Table S1. Linear models testing the influence of treatment (burned vs. unburned) plant material (leaf, stem) on sage biomass prior to addition to aquatic mesocosms. Factor interactions were excluded, except for their three-way interaction, which allowed for *a priori* contrasts of burning effects within plant tissue types in a single species.

Sage biomass	*Effect*	*SS*	*df*	*F*	*p-value*
Nitrogen (%N)	Treatment	0.028	1	8.663	**0.019**
	Type	0.260	1	80.525	**<0.001**
	Treatment:Type	0.071	1	21.810	**0.002**
	Residual	0.026	8		
Phosphorus (%P)	Treatment	0.001	1	1.968	0.198
	Type	0.008	1	19.306	**0.002**
	Treatment:Type	0.0001	1	0.144	0.714
	Residual	0.003	8		
Potassium (%K)	Treatment	0.256	1	7.616	**0.025**
	Type	0.180	1	5.357	**0.049**
	Treatment:Type	0.074	1	2.188	0.177
	Residual	0.269	8		
Sulfur (%S)	Treatment	0.0001	1	0.132	0.726
	Type	0.112	1	141.389	**<0.001**
	Treatment:Type	00004	1	0.489	0.504
	Residual	0.006	8		
Zinc (Zn ppm)	Treatment	3,073	1	2.336	0.165
	Type	3,281	1	2.494	0.153
	Treatment:Type	1,236	1	0.940	0.361
	Residual	10,524	8		

ANOVA table generated from Type-III sum of squares using *car* package in R. *SS* = sum of squares; *df* = degrees of freedom; *MS* = mean sum of squares. Significant effects ($p<0.05$) are in bold.

Table S2. Linear models testing the influence of treatment (burned vs. unburned) plant material (leaf, stem) on willow biomass prior to addition to aquatic mesocosms. Factor interactions were excluded, except for their three-way interaction, which allowed for *a priori* contrasts of burning effects within plant tissue types in a single species.

Willow biomass	*Effect*	*SS*	*df*	*F*	*p-value*
Nitrogen (%N)	Treatment	0.082	1	6.019	**0.044**
	Type	1.454	1	107.153	**<0.001**
	Treatment:Type	0.044	1	3.212	0.116
	Residual	0.095	7		
Phosphorus (%P)	Treatment	0.006	1	18.283	**0.004**
	Type	0.007	1	20.670	**0.003**
	Treatment:Type	0.001	1	2.513	0.157
	Residual	0.002	7		
Potassium (%K)	Treatment	0.068	1	8.034	**0.025**
	Type	0.264	1	31.358	**<0.001**
	Treatment:Type	0.002	1	0.173	0.690
	Residual	0.059	7		
Sulfur (%S)	Treatment	0.003	1	22.303	**0.002**
	Type	0.042	1	374.819	**<0.001**
	Treatment:Type	0.001	1	11.985	**0.011**
	Residual	0.001	7		
Zinc (Zn ppm)	Treatment	22,363	1	35.304	**<0.001**
	Type	21,956	1	34.663	**<0.001**
	Treatment:Type	5,340	1	8.431	**0.023**
	Residual	4,434	7		

ANOVA table generated from Type-III sum of squares using *car* package in R. *SS* = sum of squares; *df* = degrees of freedom; *MS* = mean sum of squares. Significant effects ($p<0.05$) are in bold.

Table S3. Model selection for percent dissolve organic carbon (DOC), total dissolved nitrogen (TDN), and total dissolved phosphorus (TDP) with candidate GAM models* assessed in each time point, corresponding to 0, 10, 31, 59, and 89 days post addition of burned or unburned plant material to experimental mesocosms. TDP was only measured at Day-31.

Metric	*Time*	*Model*	*df*	*AIC*	*ΔAIC*
DOC	Day-0	~Treatment + s(plant material, by= Treatment)	5.5	3.2	
		~Treatment + s(plant material)	4.0	1.0	
		~s(plant material)	3.1	**-0.8**	0.0
	Day-10	~Treatment + s(plant material, by= Treatment)	10.9	**146.8**	-15.2
		~Treatment + s(plant material)	6.6	157.8	
		~s(plant material)	5.5	162.0	
	Day-31	~Treatment + s(plant material, by= Treatment)	12.5	**117.7**	-40.3
		~Treatment + s(plant material)	6.3	160.0	
		~s(plant material)	5.3	158.0	
	Day-59	~Treatment + s(plant material, by= Treatment)	8.2	**64.0**	-12.1
		~Treatment + s(plant material)	4.0	69.7	
		~s(plant material)	3.0	76.1	
	Day-89	~Treatment + s(plant material, by= Treatment)	6.3	110.9	
		~Treatment + s(plant material)	5.4	109.3	
		~s(plant material)	4.4	**108.6**	0.0
TDN	Day-0	~Treatment + s(plant material, by= Treatment)	5.0	**-85.1**	-0.6
		~Treatment + s(plant material)	4.0	-83.4	
		~s(plant material)	3.0	-84.5	
	Day-10	~Treatment + s(plant material, by= Treatment)	8.9	-7.8	
		~Treatment + s(plant material)	6.2	-10.6	
		~s(plant material)	5.3	**-12.6**	0.0
	Day-31	~Treatment + s(plant material, by= Treatment)	6.3	-11.7	
		~Treatment + s(plant material)	6.9	**-18.1**	-3.0
		~s(plant material)	5.5	-15.0	
	Day-59	~Treatment + s(plant material, by= Treatment)	11.3	**-39.6**	-13.6
		~Treatment + s(plant material)	6.1	-26.2	
		~s(plant material)	5.1	-26.0	
	Day-89	~Treatment + s(plant material, by= Treatment)	7.0	**-23.7**	-6.4
		~Treatment + s(plant material)	4.8	-20.6	
		~s(plant material)	3.6	-17.4	
TDP	Day-31	Treatment + s(plant material, by=Treatment)	9.9	**100.1**	-16.8
		Treatment + s(plant material)	5.9	117.9	
		s(plant material)	4.8	116.9	

**Treatment + s(plant material, by= Treatment)* GAM has parametric terms (*Treatment*) and separate smoothers for each treatment. *Treatment + s(plant material)* GAM has a global smoother allowing for off-set intercepts according to treatments. The *s(plant material)* GAM fits a global smoother to all data. *Bold* represents the selected models. Delta AIC (*ΔAIC*) is the difference between the selected model and the global smoother model.

Table S4. Generalized additive models (GAM) testing treatment (burned vs. unburned) and factor-smooth interaction effects on dissolved organic carbon (DOC) and total dissolved nitrogen (TDN) at five time points and total phosphorous (TP) at one time point. Separate smoothers were fit for burned and unburned data, and anova tables were generated by *anova.gam*().

	Effect	*df /edf*	*Ref.df*	*F*	*p-value*
Dissolved organic carbon (DOC mg/L)					
Day-0	s(plant material)	1.040	1.080	1.341	0.240
Day-10	Treatment	1	–	9.571	**0.005**
	s(plant material) : burned	3.623	4.412	119.7	**<0.001**
	s(plant material) : unburned	3.151	3.853	149.1	**<0.001**
Day-31	Treatment	1	–	0.035	0.853
	s(plant material) : burned	6.482	7.532	34.39	**<0.001**
	s(plant material) : unburned	1.568	1.929	59.34	**<0.001**
Day-59	Treatment	1	–	12.32	**0.002**
	s(plant material) : burned	2.051	2.532	94.00	**<0.001**
	s(plant material) : unburned	2.202	2.714	56.55	**<0.001**
Day-89	s(plant material)	1.928	2.385	29.80	**<0.001**
Total dissolved nitrogen (TDN mg/L)					
Day-0	Treatment	1	–	0.879	0.357
	s(plant material) : burned	1.000	1.000	0.009	0.927
	s(plant material) : unburned	1.000	1.000	6.303	**0.019**
Day-10	s(plant material)	2.848	3.492	5.720	**0.003**
Day-31	Treatment	1	–	4.122	0.053
	s(plant material)	3.207	3.921	4.870	**0.004**
Day-59	Treatment	1	–	3.500	0.075
	s(plant material) : burned	4.359	5.269	23.03	**<0.001**
	s(plant material) : unburned	2.457	3.022	10.52	**<0.001**
Day-89	Treatment	1	–	6.231	**0.020**
	s(plant material) : burned	2.417	2.973	3.613	**0.032**
	s(plant material) : unburned	1.000	1.000	0.531	0.473
Total dissolved phosphorus (TDP μmol/L)					
Day-31	Treatment	1	–	1.329	0.267
	s(plant material) : burned	2.924	3.525	154.7	**<0.001**
	s(plant material) : unburned	2.930	3.371	124.6	**<0.001**

Treatment indicates the parametric term in GAM, *s(plant material)* is the smooth term for either burned or unburned treatments. *df / edf* column indicates either *df* (degrees of freedom) for parametric terms or *edf* (effective degrees of freedom) for smoother terms; *Ref.df* = reference degree of freedom, where dashes indicate NA for parametric terms. Significant effects ($p<0.05$) are in bold.

Table S5. Model selection for percent dissolved oxygen (DO as % O_2) with candidate GAM models* assessed in each time point, corresponding to Days-10, 31, 59, and 89 post addition of burned or unburned plant material to experimental mesocosms. Dawn and dusk measurements represent discrete back-to-back measurements over a 24 h period.

Metric	*Time*		*Model*	*df*	*AIC*	*ΔAIC*
% O_2	Day-10	dawn-1	~Treatment + s(plant material, by= Treatment)	9.7	226.4	
			~Treatment + s(plant material)	6.7	**221.5**	-3.9
			~s(plant material)	5.6	225.4	
		dusk-1	~Treatment + s(plant material, by= Treatment)	9.3	258.5	
			~Treatment + s(plant material)	6.5	**254.3**	-3.1
			~s(plant material)	5.4	257.4	
		dawn-2	~Treatment + s(plant material, by= Treatment)	9.9	230.6	
			~Treatment + s(plant material)	6.8	**228.9**	-4.7
			~s(plant material)	5.6	233.6	
	Day-31	dawn-1	~Treatment + s(plant material, by= Treatment)	8.4	**231.2**	-4.8
			~Treatment + s(plant material)	4.0	237.8	
			~s(plant material)	3.0	236.0	
		dusk-1	~Treatment + s(plant material, by= Treatment)	8.2	**246.9**	-4.3
			~Treatment + s(plant material)	4.0	251.7	
			~s(plant material)	3.0	251.2	
		dawn-2	~Treatment + s(plant material, by= Treatment)	8.8	**229.5**	-7.4
			~Treatment + s(plant material)	4.0	238.5	
			~s(plant material)	3.0	237.0	
	Day-59	dawn-1	~Treatment + s(plant material, by= Treatment)	10.0	**198.3**	-22.8
			~Treatment + s(plant material)	6.5	222.3	
			~s(plant material)	5.5	221.1	
		dusk-1	~Treatment + s(plant material, by= Treatment)	12.4	**215.3**	-22.9
			~Treatment + s(plant material)	6.9	237.2	
			~s(plant material)	5.9	238.2	
		dawn-2	~Treatment + s(plant material, by= Treatment)	10.2	**195.7**	-25.4
			~Treatment + s(plant material)	6.6	221.4	
			~s(plant material)	5.5	221.1	
	Day-89	dawn-1	~Treatment + s(plant material, by= Treatment)	6.5	208.2	
			~Treatment + s(plant material)	5.0	208.2	
			~s(plant material)	4.1	**206.3**	0.0
		dusk-1	~Treatment + s(plant material, by= Treatment)	7.1	**229.0**	-2.0
			~Treatment + s(plant material)	5.6	232.5	
			~s(plant material)	4.7	231.0	
		dawn-2	~Treatment + s(plant material, by= Treatment)	6.0	198.5	
			~Treatment + s(plant material)	4.0	196.6	
			~s(plant material)	3.1	**195.0**	0.0

**Treatment + s(plant material, by= Treatment)* GAM has parametric terms (*Treatment*) and separate smoothers for each treatment. *Treatment + s(plant material)* GAM has a global smoother allowing for off-set intercepts according to treatments. The *s(plant material)* GAM fits a global smoother to all data. *Bold* represents the selected models. Delta AIC (*ΔAIC*) is the difference between the selected model and the global smoother model.

Table S6. Generalized additive models (GAM) testing treatment (burned vs. unburned) and factor-smooth interaction effects on dissolved oxygen measured at dawn, dusk, and dawn over a 24 h period. Separate smoothers were fit for burned and unburned data, and anova tables were generated by *anova.gam*().

Dissolved oxygen (% O_2)						
		Effect	*df /edf*	*Ref.df*	*F*	*p-value*
Day-10	dawn-1	Treatment	1	–	5.467	**0.028**
		s(plant material)	3.516	4.287	127.7	**<0.001**
	dusk-1	Treatment	1	–	4.718	**0.040**
		s(plant material)	3.225	3.942	73.89	**<0.001**
	dawn-2	Treatment	1	–	6.333	**0.019**
		s(plant material)	3.481	4.245	114.0	**<0.001**
Day-31	dawn-1	Treatment	1	–	0.309	0.584
		s(plant material) : burned	1.844	2.282	32.91	**<0.001**
		s(plant material) : unburned	2.508	3.083	14.25	**<0.001**
	dusk-1	Treatment	1	–	1.887	0.182
		s(plant material) : burned	2.026	2.503	25.65	**<0.001**
		s(plant material) : unburned	2.190	2.699	10.07	**<0.001**
	dawn-2	Treatment	1	–	0.744	0.397
		s(plant material) : burned	2.289	2.818	27.35	**<0.001**
		s(plant material) : unburned	2.411	2.966	10.64	**<0.001**
Day-59	dawn-1	Treatment	1	–	1.656	0.212
		s(plant material) : burned	4.970	5.958	23.28	**<0.001**
		s(plant material) : unburned	1.000	1.000	52.88	**<0.001**
	dusk-1	Treatment	1	–	6.275	**0.021**
		s(plant material) : burned	5.038	6033	24.8	**<0.001**
		s(plant material) : unburned	2.753	3.377	14.67	**<0.001**
	dawn-2	Treatment	1	–	3.860	**0.062**
		s(plant material) : burned	5.166	6.175	22.80	**<0.001**
		s(plant material) : unburned	1.000	1.000	38.78	**<0.001**
Day-89	dawn-1	s(plant material)	1.667	2.061	9.333	**<0.001**
	dusk-1	Treatment	1	–	0.506	0.483
		s(plant material) : burned	2.575	3.163	5.636	**0.004**
		s(plant material) : unburned	1.000	1.000	2.538	0.124
	dawn-2	s(plant material)	1.041	1.081	15.09	**<0.001**

Treatment indicates the parametric term in GAM, *s(plant material)* is the smooth term for either burned or unburned treatments. *df* = degrees of freedom for parametric terms; *edf* = effective degrees of freedom for smoother terms; *Ref.df* = reference degree of freedom, where dashes indicate NA for parametric terms. Significant effects ($p<0.05$) are in bold.

Table S7. Model selection for net primary productivity (NPP) and respiration (R) with candidate GAM models* assessed at 4 time points post addition of burned or unburned plant material to experimental mesocosms.

Metric	*Time*	*Model*	*df*	*AIC*	*ΔAIC*
NPP	Day-10	~Treatment + s(plant material, by= Treatment)	8.1	214.2	-0.9
		~Treatment + s(plant material)	6.1	**213.5**	
		~s(plant material)	5.0	214.4	
	Day-31	~Treatment + s(plant material, by= Treatment)	6.4	177.5	-9.3
		~Treatment + s(plant material)	7.7	**176.3**	
		~s(plant material)	4.2	185.6	
	Day-59	~Treatment + s(plant material, by= Treatment)	11.0	175.7	-6.0
		~Treatment + s(plant material)	7.3	**175.2**	
		~s(plant material)	6.1	181.2	
	Day-89	~Treatment + s(plant material, by= Treatment)	7.4	**187.4**	-5.2
		~Treatment + s(plant material)	5.8	192.2	
		~s(plant material)	4.8	192.5	
R	Day-10	~Treatment + s(plant material, by= Treatment)	8.0	207.9	
		~Treatment + s(plant material)	6.1	203.6	
		~s(plant material)	5.1	**203.3**	0.0
	Day-31	~Treatment + s(plant material, by= Treatment)	5.0	189.6	
		~Treatment + s(plant material)	9.6	**173.3**	-6.4
		~s(plant material)	8.3	179.7	
	Day-59	~Treatment + s(plant material, by= Treatment)	11.6	**164.9**	-5.8
		~Treatment + s(plant material)	7.4	167.6	
		~s(plant material)	6.3	170.8	
	Day-89	~Treatment + s(plant material, by= Treatment)	7.5	**196.9**	-7.0
		~Treatment + s(plant material)	6.0	202.9	
		~s(plant material)	4.9	203.9	

**Treatment + s(plant material, by= Treatment)* GAM has parametric terms (*Treatment*) and separate smoothers for each treatment. *Treatment + s(plant material)* GAM has a global smoother allowing for off-set intercepts according to treatments. The *s(plant material)* GAM fits a global smoother to all data. *Bold* represents the selected models. Delta AIC (*ΔAIC*) is the difference between the selected model and the global smoother model.

Table S8. Generalized additive models (GAM) testing treatment (burned vs. unburned) and factor-smooth interaction effects on net primary productivity (NPP) and respiration (R) at 4 time points following the addition of plant material to experimental mesocosm. Separate smoothers were fit for burned and unburned data, and ANOVA tables were generated by *anova.gam*().

	Effect	*df /edf*	*Ref.df*	*F*	*p-value*
Net primary productivity (NPP Δ % O_2)					
Day-10	Treatment	1	–	2.626	0.117
	s(plant material)	2.552	3.136	15.760	**<0.001**
Day-31	Treatment	1	–	8.479	**0.007**
	s(plant material)	3.867	4.699	4.856	**0.006**
Day-59	Treatment	1	–	7.304	**0.012**
	s(plant material)	3.719	4.525	8.277	**<0.001**
Day-89	Treatment	1	–	2.620	0.118
	s(plant material) : burned	2.757	3.382	3.717	**0.020**
	s(plant material) : unburned	1.000	1.000	1.002	0.327
Respiration (R Δ % O_2)					
Day-10	Treatment	1	–	1.520	0.229
	s(plant material)	2.533	3.113	13.000	**<0.001**
Day-31	Treatment	1	–	6.443	**0.019**
	s(plant material)	5.710	6.758	10.000	**<0.001**
Day-59	Treatment	1	–	5.669	**0.027**
	s(plant material) : burned	3.762	4.576	13.144	**<0.001**
	s(plant material) : unburned	3.274	4.000	7.775	**<0.001**
Day-89	Treatment	1	–	3.380	0.078
	s(plant material) : burned	2.927	3.587	5.293	**0.004**
	s(plant material) : unburned	1.000	1.000	0.002	0.965

Treatment indicates the parametric term in GAM, *s(plant material)* is the smooth term for either burned or unburned treatments. *df* = degrees of freedom for parametric terms; *edf* = effective degrees of freedom for smoother terms; *Ref.df* = reference degree of freedom, where dashes indicate NA for parametric terms. Significant effects ($p<0.05$) are in bold.

Table S9. Non-parametric Mann-Whitney *U*-test and linear models testing effects of treatments (burned vs. unburned) and sample types (^{15}N-labeled sage, non-labeled willow, and plankton stock) on nitrogen isotope values (δ^{15}N) and C:N ratios prior to the start of the experiment (Day-0).

Mann-Whitney *U*-tests

Metric	*Material*	*Contrast*	*U*	*p-value*
δ^{15}N	Leaf material	willow *vs*. sage	315	**<0.001**
C:N			160	**0.014**
δ^{15}N	Willow, plankton	willow *vs*. plankton stock	28	**0.001**
C:N			28	**0.001**

Linear models

Metric	*Material*	*Effect*	*df*	*SS*	*MS*	*F*	*p-value*
sage-δ^{15}N	Leaf material	Treatment	2	5,178	2,589	0.913	0.423
		Residual	15	42,461	2,837		
sage-C:N		Treatment	2	3,011	1,505	11.320	**0.001**
		Residual	13	1729	133		
willow-δ^{15}N		Treatment	1	0.050	0.050	0.554	0.485
		Residual	6	0.538	0.090		
willow-C:N		Treatment	1	14.773	14.773	5.279	0.061
		Residual	6	16.789	2.798		

Sample size is *n*=7 (plankton), *n*=18 (sage), *n*=8 (willow).

Table S10. Model selection using plankton of two size classes (< 63 and >63 μm) and measuring the trophic transfer efficiency (percent of ^{15}N-labeled sage) in plankton biomass determined using a two-member mixing model and their stable isotope values ($\delta^{15}N$). Candidate GAM models* were assessed in two each time points post addition of burned or unburned plant material to experimental mesocosms.

Metric	*Time*	*Model*	*df*	*AIC*	*ΔAIC*
% sage-^{15}N	Day-10	Treatment + Type + s(plant material, by=Treatment)	12.9	**354.1**	-26.7
		Treatment + Type + s(plant material)	8.7	359.8	
		s(plant material)	6.0	380.8	
	Day-31	Treatment + Type + s(plant material, by=Treatment)	12.8	**367.5**	-24.1
		Treatment + Type + s(plant material)	8.2	385.6	
		s(plant material)	6.1	391.6	
$\delta^{15}N$	Day-10	Treatment + Type + s(plant material, by=Treatment)	12.9	**479.4**	-26.7
		Treatment + Type + s(plant material)	8.7	485.1	
		s(plant material)	6.0	506.1	
	Day-31	Treatment + Type + s(plant material, by=Treatment)	12.8	**492.7**	-24.1
		Treatment + Type + s(plant material)	8.2	510.8	
		s(plant material)	6.1	516.8	

* *Treatment + Type* represent parametric terms that provide offsets for either separate smoothers for each treatment *s(plant material, by=Treatment* or global smoothers *s(plant material)*. *Bold* represents the selected models. Delta AIC (*ΔAIC*) is the difference between the selected model and the global smoother model.

Table S11. Generalized additive models (GAM) testing treatment (burned vs. unburned) and type (< 63 μm, > 63 μm) and factor-smooth interaction effects on trophic transfer efficiency (TTE, plankton percent sage-^{15}N) calculated from a two-member mixing model. Separate smoothers were fit for burned and unburned data, and ANOVA tables were generated by *anova.gam*().

TTE, Plankton % sage-^{15}N					
	Effect	*df / edf*	*Ref.df*	*F*	*p-value*
Day-10	Treatment	1	–	31.261	**<0.001**
	Type	1	–	1.721	0.196
	s(plant material) : burned	3.560	4.338	136.8	**<0.001**
	s(plant material) : unburned	3.921	4.762	173.6	**<0.001**
Day-31	Treatment	1	–	13.082	**<0.001**
	Type	1	–	1.004	0.321
	s(plant material) : burned	4.669	5.621	79.45	**<0.001**
	s(plant material) : unburned	3.34	4.082	125.45	**<0.001**

Treatment indicates the parametric term in GAM, *s(plant material)* is the smooth term for either burned or unburned treatments. *df / edf* column indicates either *df* (degrees of freedom) for parametric terms or *edf* (effective degrees of freedom) for smoother terms; *Ref.df* = reference degree of freedom, where dashes indicate NA for parametric terms. Significant effects ($p<0.05$) are in bold.

Table S12. Model selection for greenhouse gas concentrations – carbon dioxide (CO_2 μM) and methane (CH_4 nM) – with candidate GAM models* assessed in before and 3 time point after the addition of burned or unburned plant material to experimental mesocosms.

Metric	*Time*	*Model*	*df*	*AIC*	*ΔAIC*
CO_2	Day-0	Treatment +s(plant material, by=Treatment)	8.9	**161.3**	-20.3
		Treatment + s(plant material)	4.0	176.0	
		s(plant material)	3.0	181.6	
	Day-10	Treatment +s(plant material, by=Treatment)	9.2	**271.2**	-8.1
		Treatment + s(plant material)	6.6	272.9	
		s(plant material)	5.4	279.3	
	Day-31	Treatment +s(plant material, by=Treatment)	10.2	**269.6**	-14.1
		Treatment + s(plant material)	4.0	285.4	
		s(plant material)	3.0	283.7	
	Day-59	Treatment +s(plant material, by=Treatment)	7.2	**268.0**	-8.8
		Treatment + s(plant material)	5.4	277.1	
		s(plant material)	4.3	276.8	
CH_4	Day-0	Treatment +s(plant material, by=Treatment)	5.0	132.5	-0.2
		Treatment + s(plant material)	4.0	**131.1**	
		s(plant material)	3.0	131.3	
	Day-10	Treatment +s(plant material, by=Treatment)	9.3	**159.3**	-5.3
		Treatment + s(plant material)	6.0	166.3	
		s(plant material)	5.1	164.6	
	Day-31	Treatment +s(plant material, by=Treatment)	5.9	197.8	
		Treatment + s(plant material)	4.0	196.3	
		s(plant material)	3.0	**194.9**	0.0
	Day-59	Treatment +s(plant material, by=Treatment)	5.0	227.5	
		Treatment + s(plant material)	7.1	**223.5**	-2.3
		s(plant material)	5.9	225.8	

**Treatment + s(plant material, by= Treatment)* GAM has parametric terms (*Treatment*) and separate smoothers for each treatment. *Treatment + s(plant material)* GAM has a global smoother allowing for off-set intercepts according to treatments. The *s(plant material)* GAM fits a global smoother to all data. *Bold* represents the selected models. Delta AIC (*ΔAIC*) is the difference between the selected model and the global smoother model.

Table S13. Generalized additive models (GAM) testing treatment (burned vs. unburned) and factor-smooth interaction effects on carbon dioxide (CO_2) and methane (CH_4) emissions from experimental mesocosms. Separate smoothers were fit for burned and unburned data, and ANOVA tables were generated by *anova.gam*().

Carbon dioxide (µM)					
	Effect	*df /edf*	*Ref.df*	*F*	*p-value*
Day-0	Treatment	1	–	14.980	**<0.001**
	s(plant material) : burned	1.000	1.000	10.566	**0.004**
	s(plant material) : unburned	4.022	4.880	3.383	**0.024**
Day-10	Treatment	1	–	9.403	**0.005**
	s(plant material) : burned	2.047	2.527	155.7	**<0.001**
	s(plant material) : unburned	2.966	3.633	144.2	**<0.001**
Day-31	Treatment	1	–	0.427	0.520
	s(plant material) : burned	2.499	3.072	52.20	**<0.001**
	s(plant material) : unburned	3.422	4.176	22.47	**<0.001**
Day-59	Treatment	1	–	2.341	0.140
	s(plant material) : burned	2.744	3.366	11.86	**<0.001**
	s(plant material) : unburned	1.000	1.000	28.09	**<0.001**
Methane (nM)					
Day-0	Treatment	1	–	2.038	0.166
	s(plant material)	1.000	1.000	0.718	0.405
Day-10	Treatment	1	–	0.266	0.611
	s(plant material) : burned	1.813	2.244	0.890	0.427
	s(plant material) : unburned	3.346	4.086	6.530	**0.001**
Day-31	s(plant material)	1	1.001	0.190	0.667
Day-59	Treatment	1	–	3.645	0.068
	s(plant material)	3.381	4.127	2.038	0.113

Treatment indicates the parametric term in GAM, *s(plant material)* is the smooth term for either burned or unburned treatments. *df* = degrees of freedom for parametric terms; *edf* = effective degrees of freedom for smoother terms; *Ref.df* = reference degree of freedom, where dashes indicate NA for parametric terms. Significant effects ($p<0.05$) are in bold.